

A Low-Cost, Ultra-Fine Particle Concentration Monitor

Final Report

Project ICAT 04-03

Innovative Technologies for Clean Air

California Air Resources Board

Prepared by

Susanne V. Hering

Aerosol Dynamics Inc., Berkeley, CA, 94710 USA

July 30, 2006

Disclaimer

The statements and conclusions in this report are those of the grantee and not necessarily those of the California Air Resources Board. The mention of commercial products, their source, or their use in connection with the material reported herein is not to be construed as actual or implied endorsement of such products.

Acknowledgements

We thank Jorn Herner of the California Air Resources Board, and Brian Osmondson of TSI Inc. for their interest and support, and for the loan of some of the instruments used for the comparison studies presented here. We thank Paul Ziemann of the University of California and Kenneth Docherty and Jose-Louis Jimenez of the University of Colorado for organizing and providing logistics support for the Study of Organic Aerosols in Riverside (SOAR), and Melissa Lunden for having made her house available for these studies. We thank Brent Williams of the University of California Berkeley who provided a watchful eye during the Riverside measurements when we could not be present.

Most especially, we thank Frederick Quant, Dereck Oberreit and Patricia Keady of Quant Technologies LLC, who transformed our concepts into the Micro-Environmental Water-based Condensation Particle Counter tested here. Their enthusiasm and dedication throughout this project, and their commitment to good engineering design was critical to the success of this instrument.

Table of Contents

Acknowledgements	ii
List of Figures	iv
List of Tables	vi
Abstract	vii
Introduction	1
Instrument Description	2
Theory of Operation	4
Experimental Evaluation Methods	5
Results	
Size-Dependent Detection Efficiency	10
Response to Aerosols of Known Composition	10
Ambient Measurements	13
Indoor Measurements	13
Comparisons Among Instruments	18
Summary	23
References	24
Appendix A	26

List of Figures

Figure 1.	Photograph of the Micro-environmental, Water-based Condensation Particle Counter (ME-WCPC).	3
Figure 2.	Flow schematic of the micro-environmental water-based condensation particle counter (ME-WCPC), showing conditioner, growth tube, porous media used for wick, and optics head.	3
Figure 3.	Contour lines of equal water saturation within the water CPC growth tube for a 40°C temperature difference between the growth tube walls and the entering flow.	4
Figure 4.	Schematic of the “CPC Array”, with collocated sampling from 8 different condensation particle counters, including three butanol instruments (TSI-3022, TSI-3010, TSI-3025) and five water-based instruments (TSI-3785, TSI-3786, and three prototype ME-WCPCs).	7
Figure 5.	The “CPC array” as deployed for ambient measurements in Berkeley, CA.	8
Figure 6.	Size dependent detection efficiency of the ME-WCPC, as measured with monodisperse aerosols.	10
Figure 7.	Response to broadly-classified (35% mobility window) oleic acid (top) and NaCl (bottom) aerosols, relative to that for the Ultrafine Butanol CPC (TSI-Model 3025) corrected for its efficiency at the median particle diameter, as reported by Stolzenburg and McMurry (1991).	11
Figure 8.	Response of individual CPCs in the CPC array to the TSI-3022 butanol instruments for a broadly dispersed ammonium sulfate aerosol obtained by classification with a 35% mobility window.	12
Figure 9.	Diurnal patterns in ambient particle number concentrations in July and November, 2005, in Riverside, CA as measured by different condensation particle counters.	14
Figure 10.	Diurnal patterns in ambient particle number concentrations in December 2005 and early January, 2006, in Berkeley, CA., as measured by different condensation particle counters.	15
Figure 11.	Ambient particle number concentrations on the afternoon of October 17, 2005, in Berkeley, CA., as measured by different condensation particle counters.	15
Figure 12.	Diurnal patterns in ambient particle number concentrations in an office, and in an unoccupied home in Berkeley, CA, as measured by different condensation particle counters.	16

List of Figures (continued)

Figure 13. Measurements in a residential kitchen and in a bedroom hallway, showing dramatic increases in particle number concentrations coincident with the use of a gas-fired oven. Data are from the kitchen of Residence 1 (top and middle) and the bedroom wing hallway in Residence 2 (bottom).	17
Figure 14. Scatterplots comparing the response of collocated ME-WCPC units during the Riverside and December ambient measurement periods.	19
Figure 15. Scatterplots comparing the response of the ME-WCPC unit to that of the butanol-based TSI-3022 for ambient measurements in Riverside and Berkeley, California.	19
Figure 16. Comparison of the ME-WCPC and the dilution-corrected, single-count mode butanol-based TSI-3010 to the photometric, butanol-based TSI-3022. Data are from a residential kitchen, wherein the TSI-3010 was operated with a passive 60x dilution.	21
Figure 17. Comparison of the ME-WCPC and the butanol-based TSI-3025 to the TSI-3022 operated with an 8-fold dilution.	22
 <i>Appendix Figures</i>	
Figure A1 Scatter plot of collocated ME-WCPCs, Riverside measurements	27
Figure A2 Scatter plot of collocated ME-WCPCs, Berkeley measurements	28
Figure A3 Scatter plot of collocated ME-WCPCs, indoor measurements	29
Figure A4 Comparison of the ME-WCPC to a butanol CPC for summertime measurements in Riverside	30
Figure A5 Comparison of the ME-WCPC to a butanol CPC for winter measurements in Riverside	31
Figure A6 Comparison of the ME-WCPC to a butanol CPC for fall measurements in Berkeley	32
Figure A7 Comparison of the ME-WCPC to a butanol CPC for winter measurements in Berkeley	33
Figure A8 Comparison of the ME-WCPC to a butanol CPC for indoor measurements in Berkeley	34

List of Tables

Table 1.	Instruments Operated During Each Study Period	6
Table 2.	Characteristics of Condensation Particle Counters (CPC) Utilized in the ICAT Field Evaluation	7
Table 3.	Comparisons for Collocated ME-WCPC Units	18
Table 4.	Pairwise Comparisons Among Instruments	20

Abstract

A water-based, micro-environmental condensation particle counter (ME-WCPC) has been developed to provide monitoring of particle number concentrations in ambient air and in occupied spaces. Reported here is the evaluation of this instrument under field conditions. Comparison is made to three types of butanol-based counters (TSI Models 3010, 3022, 3025) and to bench-scale water based counters (TSI Models 3785 and 3786). Ambient sampling was performed in the summer and winter in Riverside and in the winter in Berkeley, CA. Indoor measurements were made in one office and two homes, including one kitchen. At all locations the collocated ME-WCPCs agreed with each other, with the square of the correlation coefficient above 0.97 and slopes near 1. For particle number concentrations below 200,000 cm^{-3} , measurements from the ME-WCPC are within 10% percent of those from the butanol-based TSI-3022, and higher than those from the dilution-corrected TSI-3010, consistent with the differences in the lower particle size limits cutpoints of the instruments (7 nm for the TSI-3022, 10 nm for the TSI-3010). Differences among all instruments are observed at concentrations above 200,000 cm^{-3} . At all locations the ambient particle number concentrations exhibited a consistent diurnal pattern during each multi-week study period, with a dominant morning maximum and a secondary late afternoon maximum. In some cases, a third maximum is seen shortly after midnight. Indoor particle number concentrations appear to be dominated by indoor, rather than outdoor sources. Residential particle number concentrations associated with cooking activities were a factor of 10 or more higher than the highest levels observed outdoors.

A Low-Cost, Ultra-Fine Particle Concentration Monitor

Introduction

Ultra-fine particles have been associated with adverse health risks¹⁻⁴, yet their concentrations in occupied spaces are not well known. Levels in homes, offices and schools are influenced by both indoor and outdoor sources⁵⁻⁹, as well as building ventilation and proximity to roadways¹⁰⁻¹¹. Monitoring of these micro-environments where people spend the majority of their time is important for the assessment of community exposures.

For the last thirty years, ultra-fine particle number concentrations have been measured using butanol- or isopropanol-based condensation particle counters. These laminar-flow instruments provide continuous flow, and a well-defined lower particle size detection limit. Often these counters serve as detectors for electrical mobility measurements of particle size distributions. However, for reasons of odor and toxicity, they are not suitable for measurement in occupied spaces, or in many monitoring networks where worker exposure is of concern.

Recently a water-based “growth tube” technology was introduced which enables detection of ultra-fine particles in a continuous, laminar flow without using toxic substances¹². The first water-based condensation particle counter utilizing this principle was introduced in 2003. This instrument, the “standard” WCPC, detects particles as small as 5 nm¹³. The following year, an ultrafine-WCPC was introduced which employs larger temperature differences and a sheath flow, and is capable of detecting particles as small as 2.5 nm¹⁴.

Most recently, the WCPC technology has been adapted to a compact, lower-cost, micro-environmental monitor (ME-WCPC). This instrument is designed to accommodate high concentrations as can be found in urban air near combustion sources, or inside buildings and homes as a result of cooking or heating. The ME-WCPC is designed with single particle counting throughout its entire range in particle concentration, from 1 cm⁻³ to 5 x 10⁵ cm⁻³. This is done to avoid the reliance on an empirical, photometric calibration as is often used for high concentration measurement. Additionally, an effort has been made to reduce its size and fabrication cost. Importantly, because the condensing vapor is water, it can be operated in occupied spaces or in monitoring locations where the butanol is a hazard.

This report presents a description and field evaluation of the ME-WCPC, with comparison to both butanol-based and standard, bench-scale water-based condensation particle counters. Data are presented from ambient measurements in Riverside and Berkeley, California, and from measurements in two homes and one office.

Instrument Description

Shown in Figure 1, the micro-environmental, water-based condensation particle counter (ME-WCPC) measures 18 cm x 13 cm x 25 cm including fill bottle, and weighs 2.3 kg. It operates on 30 W of 12-Volt power, and has an external power supply for conversion from 100-240 VAC, 50/60 Hz. In addition to serial output, the instrument has internal data logging with a date/time stamp provided by an internal, battery-sustained clock. The 4 megabits of internal memory is capable of storing two weeks of one-minute data. The water fill bottle is sized to provide one week of unattended operation.

Figure 2 gives the instrument schematic. Air is brought into the instrument at 0.6 L/min, of which 0.12 L/min is sample flow and 0.48 L/min is transport flow used to reduce diffusional losses at small particle sizes. The sample air stream passes in a laminar flow through the conditioner and growth tube, then through a focusing nozzle into the optics head, and exits through a metering orifice used to control the sample flow rate. After the metering orifice, the transport flow mixes with the exiting sample flow to reduce the water vapor pressure.

The conditioner and growth tube are lined with a porous “wick” which is constantly wetted by contact with the internal water reservoir. A float valve is used to activate the fill valve to maintain the water level in the internal reservoir. The walls of the conditioner are held at 20°C by means of a thermo-electric device. The walls of the growth tube are heated to 60°C, and are continually wetted by the wick. Because the mass diffusivity of water vapor is higher than the thermal diffusivity of air, the transport of water vapor from the heated walls into the particle-laden stream is faster than the increase in temperature. This creates a region of supersaturation inside the growth tube, and subsequent particle growth by condensation. Once enlarged the particles are detected optically.

The droplets formed by condensational growth pass through a light beam in the optics head. At low particle concentrations, each particle produces a light-scattering pulse which is detected by the photodetector. These are individually counted, and together with the aerosol sample rate yield the particle number concentration. At higher particle concentrations, it is necessary to account for coincidence. This is equivalent to accounting for dead time, defined as the time occupied by the particle while it is in the light beam, blocking the detection of any incoming particles.

For each 100 ms interval, the WCPC tracks the number of light-scattering pulses and the discriminator time, defined as the time during which the photodetector signal is above the lower threshold. The particle concentration is calculated using the ratio of the number of pulses detected (or “counts”) to the effective “live time”, defined as the difference between the clock time and the effective dead time. For the WCPCs, the effective dead time is estimated as the measured discriminator time multiplied by an empirically determined dead time correction factor, as discussed by Hering et al¹³. This dead time correction factor accounts for the overlapping below the detector threshold level of the tails of the light scattering pulses, which reduces beyond the measured dead time the time window during which the photodetector is available for detecting incoming particles. Dead time correction factors are determined empirically for each unit by calibration with a 50-60 nm NaCl aerosol.



Figure 1. Photograph of the Micro-environmental, Water-based Condensation Particle Counter (ME-WCPC)

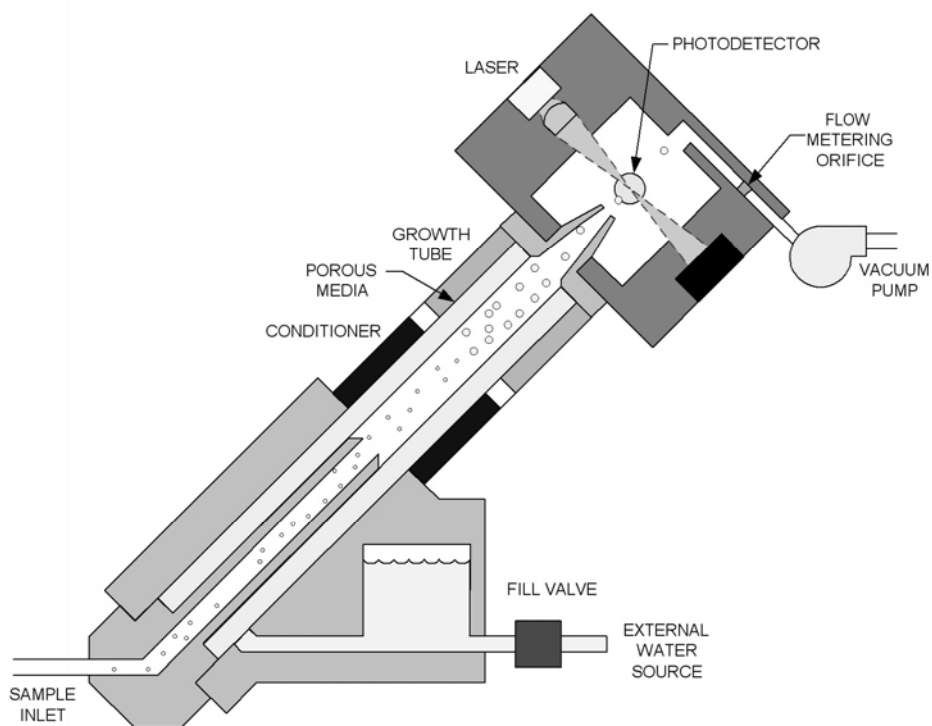


Figure 2. Flow schematic of the microenvironmental water-based condensation particle counter (ME-WCPC), showing conditioner, growth tube, porous media used for wick, and optics head.

Theory of Operation

Because ultrafine particles are too small to be measured directly by optical means, condensation particle counters first enlarge these particles through condensation. For small particles, the activation of the condensational growth requires the creation of a region of vapor supersaturation. Because of surface tension, the equilibrium vapor pressure for a water droplet is higher than over a flat surface, an effect described by the Kelvin relation. Solute effects, as described by the Kohler equation, also play a role. Whatever the particle chemical composition, for small particles the activation of particle growth requires the creation of a region of supersaturation. The higher the supersaturation, the smaller the particle of that type that is activated to grow.

With alcohol-based counters, a region of alcohol-vapor supersaturation is created by flowing the sample stream over an alcohol saturated surface, and into a cold-walled tube. This approach requires a slowly diffusing vapor, such that the flow cools faster than the vapor diffuses to the walls of the condenser. It does not work well with water, which has a mass diffusivity which is larger than the thermal diffusivity of air. With the WCPC the temperatures are reversed – a cold flow is introduced into a warm, wet-walled “growth tube”. This non-intuitive approach accounts for the fact that the mass diffusivity of water vapor exceeds the thermal diffusivity of air. The elevated temperature of the wetted walls produces a high concentration of water vapor, while the “cooling” arises from the entering sample air flow.

Calculated supersaturation profiles for the ME-WCPC are shown in Figure 3. These are based on the work of Stolzenburg and McMurry¹⁵, as adapted to the growth tube by Hering and Stolzenburg¹². Also shown is the Kelvin-equivalent diameter of the smallest particles that are activated to grow. Note that the maximum supersaturation is achieved along the centerline, which carries the majority of the flow.

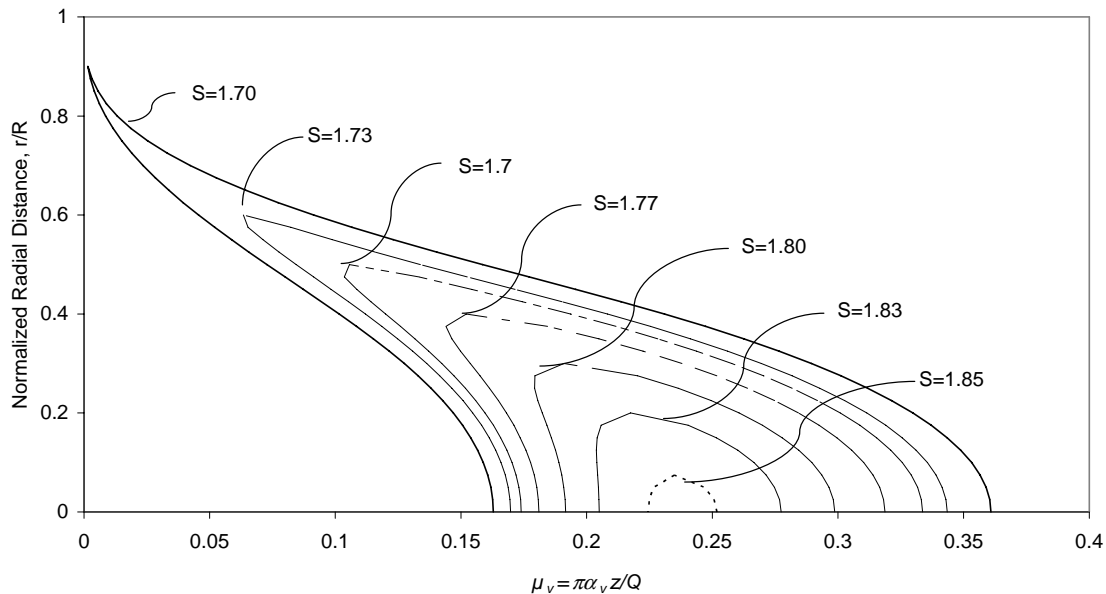


Figure 3. Contour lines of equal water saturation within the water CPC growth tube for a 40°C temperature difference between the growth tube walls and the entering flow. The profiles scale as the Peclet number, $\pi\alpha_v Z/Q$, where α_v is the vapor diffusivity; z is axial position and Q is the volumetric flow rate. R = tube radius; r = radial position.

Experimental Evaluation Methods

Four separate sets of ambient tests, and three sets of indoor tests were conducted, as outlined in Table 1. Ambient measurements in Riverside California were conducted from July 27 through August 14, 2005, and again from October 27 through November 22, 2005 in conjunction with the Study of Organic Aerosols in Riverside (SOAR). The monitoring site was located in a parking area on the campus of the University of California, 0.5 km northeast of the Interstate freeway carrying an average of 180,000 vehicles per day. Measurements in Berkeley were conducted between the two Riverside studies (October 12 – 22, 2005) and immediately afterwards (December 15, 2005 – January 6, 2006). The ambient Berkeley measurements were made from our laboratory, located 0.8 km east of the Interstate Freeway, with average traffic volumes of 290,000 vehicles per day, peaking at 18,000 per hour. Indoor measurements were conducted in one office, and two homes, all in Berkeley.

The field evaluation was conducted with an array of CPCs, as illustrated in Figure 4. Each study included several ME-WCPCs, standard or ultrafine WCPCs, and two or three types of butanol-based CPCs, as listed in Table 1. The actual units used for comparison varied among the studies, as noted by their respective serial numbers. In most cases we collocated three ME-WCPCs, so that both the precision and accuracy of the units could be tested. The bench scale WCPCs were either production units borrowed from TSI (Models 8785 and 8786), or were prototypes for these instruments, (Quant Models 400 and 410 respectively). The summer field testing was done with just two butanol CPCs; the TSI Model 3010 and the TSI 3025 ultrafine CPC. For subsequent tests, a TSI Model 3022 was added in order to have an instrument capable of high concentration measurements, yet with approximately the same nominal lower size detection efficiency as the ME-WCPC.

Characteristics of the units compared are summarized in Table 2. The instruments differ not only in working fluid (water or butanol), but in the smallest detectable particle size, the upper concentration limit, and the aerosol flow rate. The two instruments labeled “ultrafine” detect particles as small as 3 nm, while the TSI-3022 and 3010 butanol instruments have detection limits of 7 nm and 10 nm respectively. At high concentrations, the TSI-3022 utilizes a “photometric” mode, from which the total particle concentration is inferred from the scattering from the “cloud” of droplets within the detection volume. Photometrically determined concentrations are based on empirical calibration done by the manufacturer with sodium chloride aerosol. The Model 3010 butanol CPC derives concentrations from single-particle counting only, that is, by enumeration of the light scattering pulses from individual particles. While reliable, this has an upper concentration limit of 10^4cm^{-3} . For this reason the TSI-3010 was operated with a passive dilution system wherein a portion of the sample flow passes through a small orifice, while the remaining sample flow passes through a larger orifice followed by a filter to remove particles prior to entering the CPC.

A note on nomenclature is relevant. For atmospheric measurements, the term “ultrafine” is used to refer to particles with diameters less than about 100 nm. Yet, when describing condensation particle counters, the term “ultrafine” refers specifically to those instruments capable of detecting particles in the 3 to 5 nm diameter size range. According to atmospheric

Table 1. Instruments Operated During Each Study Period

Study	Start	Stop	Type of CPC	Instruments Operated (Make, Model and Serial Number)
Riverside Summer Study	7/19/2005	8/14/2005	water:	ME-WCPC, SN 104, 105, 106 Quant 400, SN 110 (equiv. to TSI-3785) Quant 410, SN 102 (equiv. to TSI-3786)
			butanol:	TSI-3010, SN 2259 TSI-3025, SN 1282&1284
Berkeley Fall Study	10/13/2005	10/22/2005	water:	ME-WCPC, SN 104, 105, 106 Quant 400, SN 110 TSI-3786, SN 70508107
			butanol:	TSI-3022, SN 70502245 TSI-3010, SN 2259 TSI-3025, SN 1284
Riverside Winter Study	10/27/2005	11/22/2005	water:	ME-WCPC, SN 104, 105, 106 TSI-3785, SN 78417542 TSI-3786, SN 70508107
			butanol:	TSI-3022, SN 70502245 TSI-3010, SN 2259 TSI-3025, SN 1284
Berkeley Winter Study	12/12/2005	1/6/2006	water:	ME-WCPC, SN 105, 106 TSI-3785, SN 78417542 Quant 410, SN 102
			butanol:	TSI-3022, SN 70502245 TSI-3010, SN 2259 TSI-3025, SN 1049
Kitchen, Residence 1	1/7/2006	1/9/2006	water:	ME-WCPC, SN 105, 106 TSI-3785, SN 78417542 Quant 410, SN 102
			butanol:	TSI-3022, SN 70502245 TSI-3010, SN 2259 TSI-3025, SN 1049
Office	5/25/2006	6/3/2006	water:	ME-WCPC, SN 104, 105 Quant 400, SN 110
			butanol:	TSI-3022, SN 321
Kitchen, Residence 1	6/3/2006	6/7/2006	water:	ME-WCPC, SN 104, 105, 106
"	6/19/2006	7/3/2006		Quant 400, SN 109
			butanol:	TSI-3022, SN 321 TSI-3010, SN 2259
Hallway, Residence 2	6/7/2006	6/16/2006	water:	ME-WCPC, SN 104, 105, 106 Quant 400, SN 109
			butanol:	TSI-3022, SN 321 TSI-3010, SN 2259

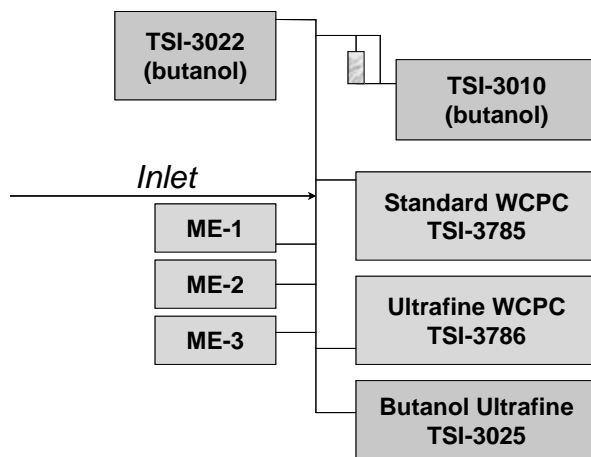


Figure 4. Schematic of the “CPC Array”, with collocated sampling from 8 different condensation particle counters, including three butanol instruments(TSI-3022, TSI-3010, TSI-3025) and five water-based instruments (TSI-3785, TSI-3786, and three prototype ME-WCPCs)

Table 2. Characteristics of Condensation Particle Counters (CPC) Utilized in the ICAT Field Evaluation

Instrument	Flow (L/min)	Lower Dp (nm)	Max Concentration	Counting Method
ME-WCPC (prototype to TSI-3781)	0.12	~5	500,000 / cm ³	dead-time corrected single particle counting
Standard WCPC (TSI-3785 or Quant-400)	1.0	5	30,000 / cm ³	dead-time corrected single particle counting
Ultrafine WCPC (TSI-3786or Quant 410)	0.3	2.5	100,000 / cm ³	dead-time corrected single particle counting
Photometric Butanol CPC (TSI-3022)	1.5	7	10,000 / cm ³ 10,000,000 / cm ³	single particle counting photometric
Standard Butanol CPC (TSI-3010)	1.0	10	10,000 / cm ³	single particle counting
Ultrafine Butanol CPC (TSI-3025)	0.03	3	100,000 / cm ³	single particle counting

usage, all CPCs are “ultrafine” counters, as they all count particles in the 10 to 100 nm size range. However, consistent with the manufacturer’s nomenclature, only the two 3-nm instruments in Table 2 are called “ultrafine”.

At Riverside instruments were deployed in a trailer, and sampled from a common 8 m-long, 8 mm ID copper sampling line equipped with a metal mesh screen at the inlet. A size-selective inlet was not employed. The plenum from which individual instruments sampled was fabricated from stainless steel Swagelok tees sized to provide laminar flow throughout the system ($Re < 1000$). Connection to the individual instruments was made by means of 6 mm OD conductive tubing. The length of the individual tubes was sized in proportion to the instrument sample rates in order to equalize diffusional losses. The calculated penetration of aerosol through the system is 75% at 5 nm, and 90% at 10 nm.

The sampling setup for ambient measurements in Berkeley is shown in Figure 5. Here the ambient measurements were made from our second-floor laboratory, with a 4 m, electrically conductive sampling line to the outside. Calculated diffusional losses were 7% at 10 nm. The sampling plenum and line length to the individual CPCs was the same as in the Riverside measurements. Office measurements were made in our Berkeley office, with a 8 m sampling line from the laboratory into the office space. This sampling line was located at a height of 1.5 m, at a distance of 2 m from the door to the laboratory and a distance of 7 m from the office laser-printer.

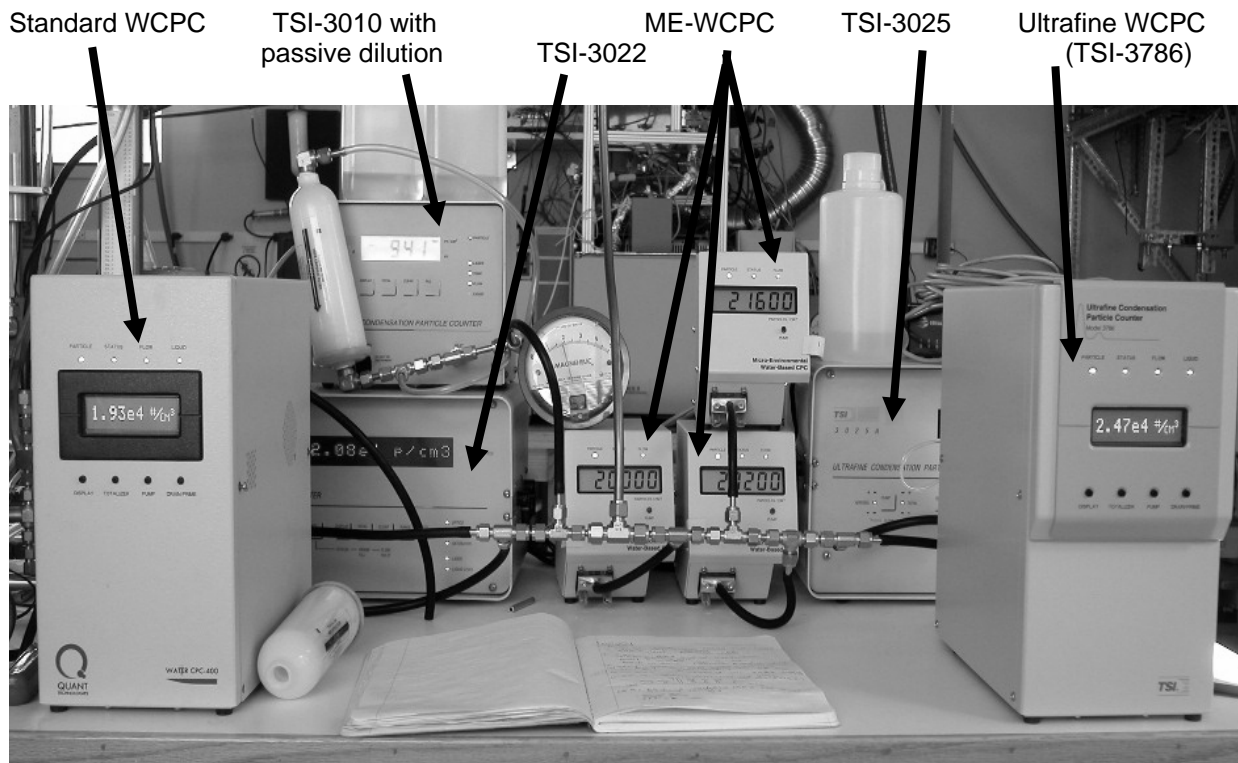


Figure 5. The “CPC array” as deployed for ambient measurements in Berkeley, CA.

In residence 1 the instruments sampled from a common inlet placed 1.5 m above floor level, 0.25 m away from the wall, and at a distance of 3 m from the stovetop. This mimics the breathing zone of someone in the kitchen, but not directly next to the stovetop. In residence 2, measurements were made from the bedroom wing of the house, with sampling from the hallway at a height of 1 m above floor. This hallway connected the bedrooms to the common kitchen and living area. In both cases, the sampling line was 3 m long.

Data were logged via a laptop computer equipped with a serial port adapter to handle 8 serial input lines. A Labview program written in-house received and date-time stamped all incoming data records. This provided a common date time mark for all systems. All data were recorded in Pacific Standard Time. The files from the 5 water-based instruments contained 5 or 6 second average concentrations, and were datetime stamped at the time data were transmitted, ie at the end of the 5 (or 6) second averaging interval. For the first two deployments, the data from the butanol-based instruments were instantaneous (1second) readings of the display. Thereafter, measurements for the TSI-3025 were obtained by dumping the 1-s buffer, which allowed recording of dead-time corrected concentrations above the nominal upper bound of 10^5cm^{-3} .

During the study the instrument flow rates were checked by means of a bubble flow meter, and the instrument “zeros” were verified by placing a HEPA filter at the inlet. For the most part instruments were operated unattended.

The relative response of the instruments was also checked with laboratory-generated sodium chloride, oleic acid and ammonium sulfate aerosols. These were generated by nebulization and size selected by using the “long” differential mobility analyzer (TSI Model 3081). These tests were used to confirm the equivalency of the instrument performance at larger particle sizes, above 20 nm. Additionally, the size-dependent response of the ME-WCPC was evaluated in the laboratory using a glucose aerosol generated by electrospray, and size-selected with a nano-differential mobility analyzer. Detection efficiencies are derived by comparison to a Model TSI-3786 ultrafine water CPC. Tests were also conducted with size-selected ambient aerosols, with comparison to a TSI-3025 ultrafine butanol CPC.

Results

Size-Dependent Detection Efficiency

Figure 6 shows the size-dependent counting efficiency for the prototype ME-WCPC, as determined by laboratory-generated sucrose aerosols. Also shown are data for size-selected ambient aerosols. The data show a 50% counting efficiency at approximately 6 nm. The activation curve is not as steep as the standard WCPC, reaching 90% detection efficiencies at 20 nm. Data for size-selected ambient aerosols are similar to that for the sucrose.

Response to Aerosols of Known Composition

As a quality assurance check, the response of the CPC array from the Riverside Summer Study was checked with aerosols of known composition generated by nebulization and broadly size-selected aerosols using a “long” DMA column operated with a 35% mobility window. Figure 7 shows the response of each instrument relative to that for the butanol UCPC (TSI-3025), corrected for the published efficiency of that instrument at the median particle diameter¹⁵. For the Model 3010 and standard WCPC the asymptotic concentrations at large particle size are normalized to those for the TSI-3025, with corresponding adjustments of 9% and 20% to the raw data, respectively. Data for the ME-WCPC units, and for the ultrafine WCPC are reduced using the measured sample flow rates.

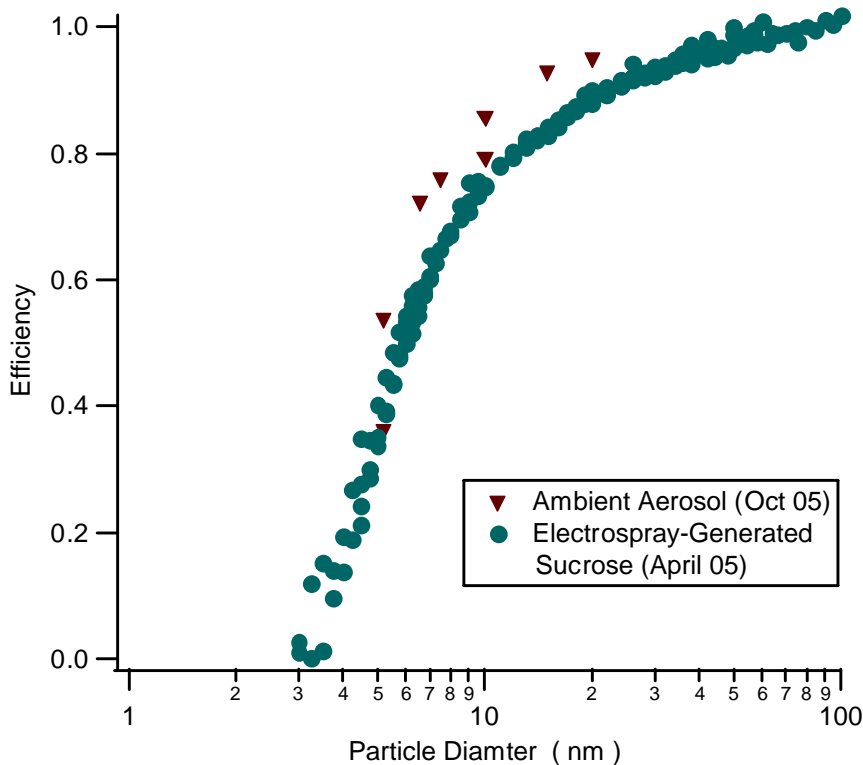


Figure 6. Size dependent detection efficiency of the ME-WCPC, as measured with monodisperse aerosols.

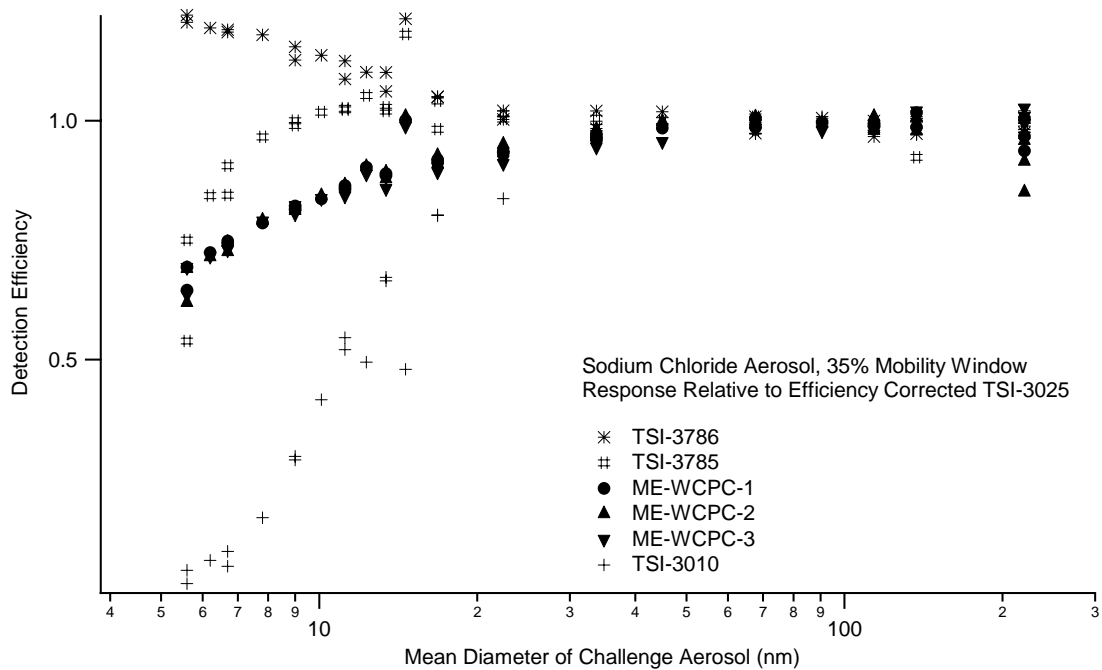
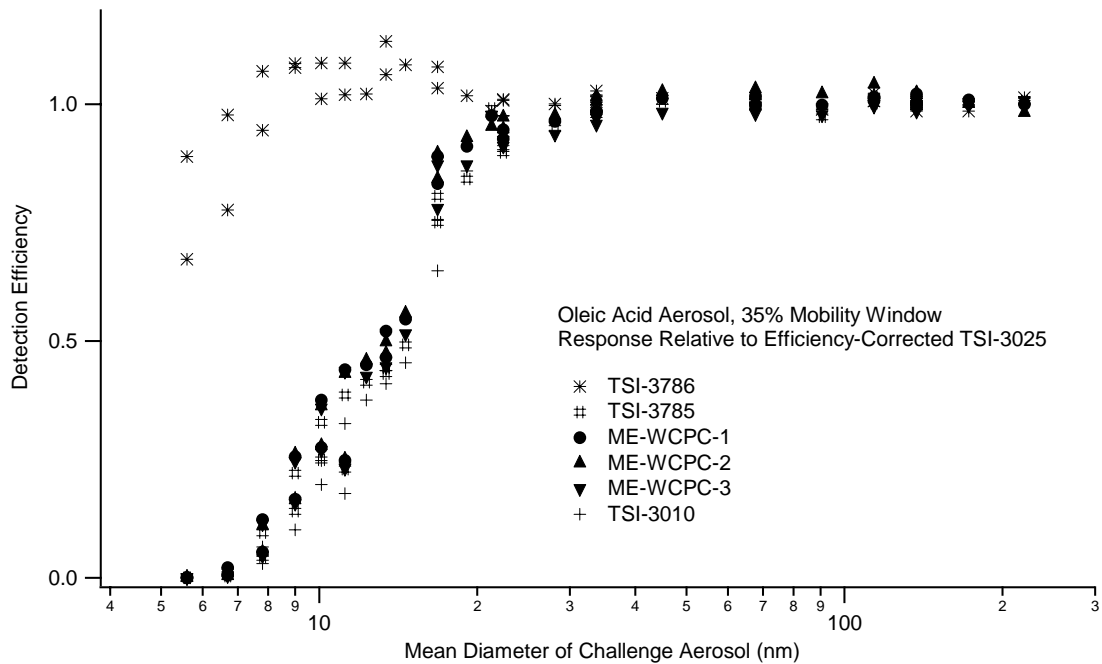


Figure 7. Response to broadly-classified (35% mobility window) oleic acid (top) and NaCl (bottom) aerosols, relative to that for the Ultrafine Butanol CPC (TSI-Model 3025) corrected for its efficiency at the median particle diameter, as reported by Stolzenburg and McMurry¹⁵. Data are plotted as a function of the median diameter of the challenge aerosol.

The data of Figure 7 cannot be interpreted as a cutpoint curve because the challenge aerosol is not monodisperse. Yet fundamental differences between the instruments are apparent. For the oleic acid aerosol, a nonhygroscopic organic material, the responses of the ME-WCPC and the standard WCPC are similar to each other, and to those of the TSI-3010. The ultrafine-WCPC responds at much smaller particle sizes. For NaCl aerosol, both the standard and ultrafine WCPCs exhibit a greater response than the TSI-3025 for the smallest particle sizes tested. This is a result of the greater detection efficiency of the WCPC for salt aerosols at very small particle sizes¹³. Overall, the ME-WCPC has somewhat lower detection efficiency than its counterpart, the standard WCPC, even though the operating temperatures are the same. This is attributed in part to an increase in the diffusional losses at the lower sampling rate of the ME-WCPC.

Figure 8 shows the response of the CPC array that was deployed in the winter studies in Riverside and Berkeley. The challenge aerosol is broadly dispersed ammonium sulfate, with a 35% mobility window. The data have been normalized to the TSI-3022 at a diameter of 100 nm, but in no case was this adjustment more than 5%. As is apparent, all of the water-CPC units (TSI-3785 and TSI-3786, and all of the ME-WCPCs) are more efficient than the butanol instruments at small particles sizes. This is similar to the results for NaCl aerosol from Figure 7 above.

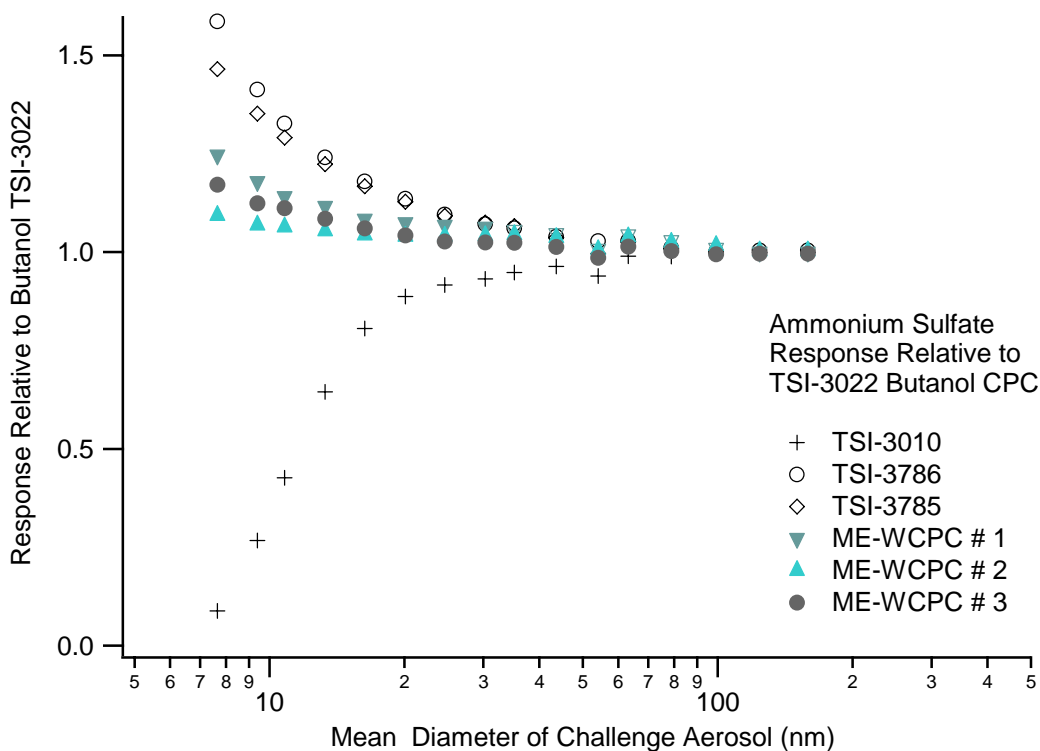


Figure 8. Response of individual CPCs in the CPC array to the TSI-3022 butanol instruments for a broadly dispersed ammonium sulfate aerosol obtained by classification with a 35% mobility window.

Ambient Measurements

The ambient particle number concentrations often exhibited a consistent diurnal pattern. Figure 9 presents the daily pattern observed for the summer and winter study periods in Riverside. Shown is the average of one-minute data at each time of day across all days in the study period. In both cases, the measurements among all instruments are highly correlated. A consistent daily pattern is apparent, with a morning rush hour maximum between 6 and 9 am, followed by a midday minimum and a smaller afternoon maximum. In the summer the afternoon maximum is broad, and coincides with the time of day when Riverside sees transport from the upwind areas of Los Angeles.

Diurnal patterns for measurements in Berkeley in December are shown in Figure 10. Daily averaged maximum concentrations for this near-freeway site are $40,000 \text{ cm}^{-3}$, with peak values reaching $2 \times 10^5 \text{ cm}^{-3}$. This is higher than seen in Riverside, where the average daily maxima was approximately $25,000 \text{ cm}^{-3}$ for both the summer and winter, with maximum concentrations of $9 \times 10^4 \text{ cm}^{-3}$. As in Riverside, the morning hour traffic peak is apparent, and is more pronounced than the evening traffic commute. In the December period a third maximum is seen occurring just after midnight, perhaps associated with the decreased ventilation at night.

Ambient measurements made in Berkeley in October did not exhibit a consistent diurnal pattern. Rather the data showed large spikes in concentration on some afternoons, presumably resulting from the proximity of large vehicles. An example from one afternoon is given in Figure 11, with concentrations in excess of $200,000 \text{ cm}^{-3}$. All of the instruments track, with the exception of the TSI-3025 which does not display concentrations in excess of 10^5 . For subsequent measurements the data acquisition program was changed to directly read the one-second buffer of this instrument, rather than the displayed concentration, so as to assess the instrument response at higher concentrations.

Indoor Measurements

Figure 12 shows diurnal profiles obtained for measurements in an office space, and in an unoccupied home. Overall, the concentrations are much lower than seen in the ambient air, with maximum concentrations below $20,000 \text{ cm}^{-3}$ in the office, and below $10,000 \text{ cm}^{-3}$ in the unoccupied home. In contrast to the ambient measurements, the office space shows a maximum concentration near noon, coincident with activity in the space. There is no indication of influence from the morning traffic commute hour. These patterns point to the importance of indoor sources and activities to indoor particle number concentrations. During all study periods the data among all instruments is well-correlated. The data from the ME-WCPC and the TSI-3022 butanol CPCs, which have detection limits near 7 nm, are similar. Likewise, the ME-WCPC data is similar to that from the “standard”, bench-scale WCPC, which has a 5 nm lower cutpoint. The two “ultrafine” instruments, the TSI-3786 water-CPC and the TSI-3025 butanol CPC, show higher concentrations than the other instruments. This is consistent with their lower 3 nm cutpoint, as compared to the 5 to 10 nm cutpoints for the other CPCs.

Measurements in a residential kitchen (Residence 1) were made in January, and again in June, 2006. As shown in Figure 13, the data show sharp peaks arising from cooking, with indicated number concentrations in excess of $10^6/\text{cm}^3$ when the gas-fueled stove top or oven

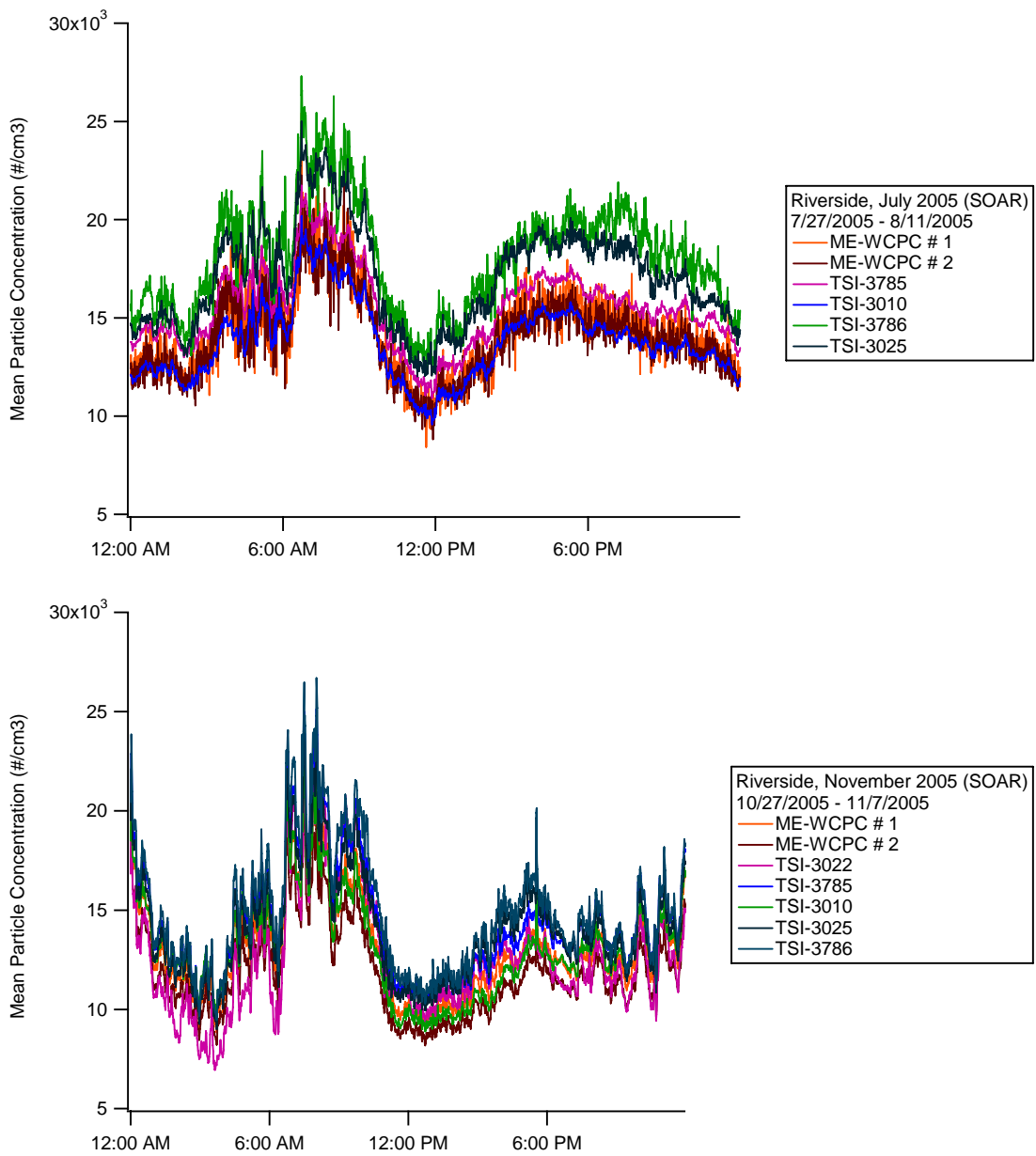


Figure 9. Diurnal patterns in ambient particle number concentrations in July and November, 2005, in Riverside, CA., as measured by different condensation particle counters.

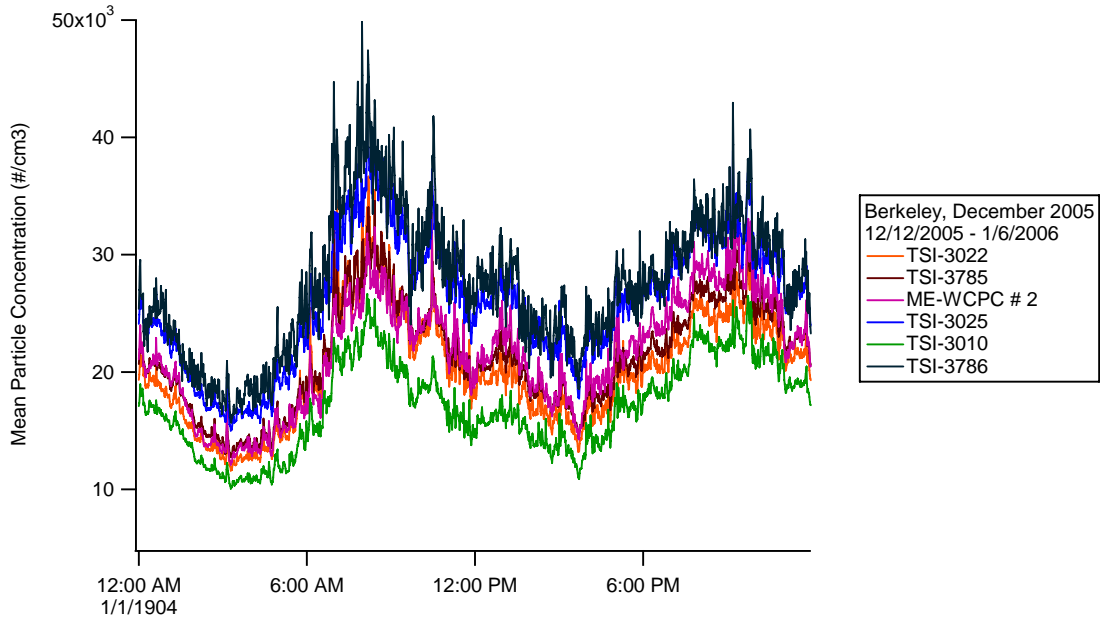


Figure 10. Diurnal patterns in ambient particle number concentrations in December 2005 and early January, 2006, 2005, in Berkeley, CA., as measured by different condensation particle counters.

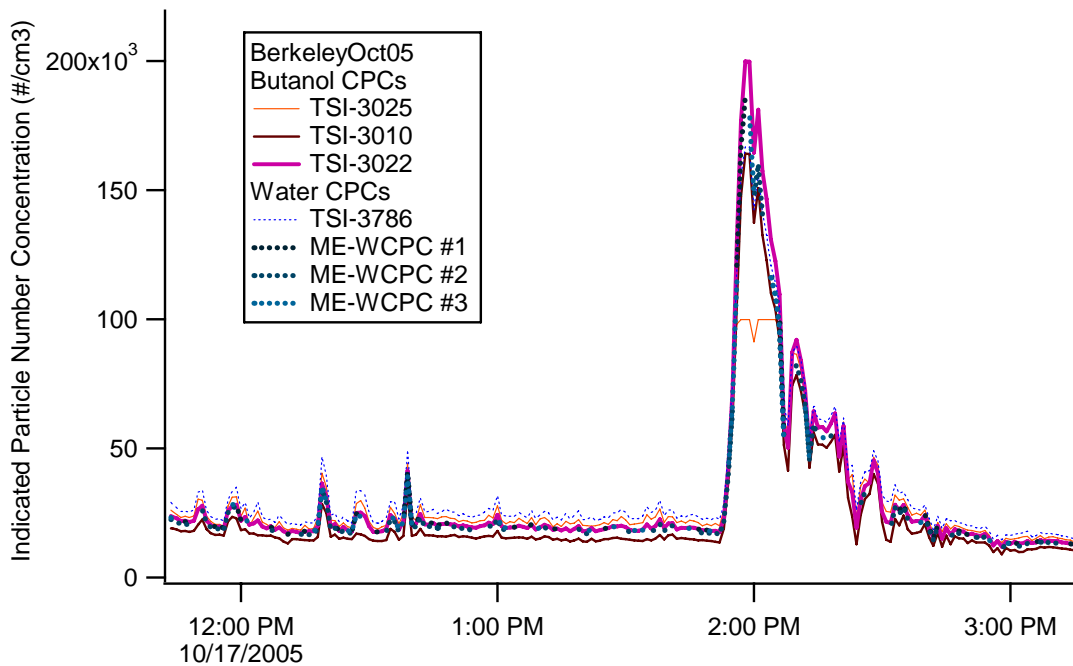


Figure 11. Ambient particle number concentrations on the afternoon of October 17, 2005, in Berkeley, CA., as measured by different condensation particle counters.

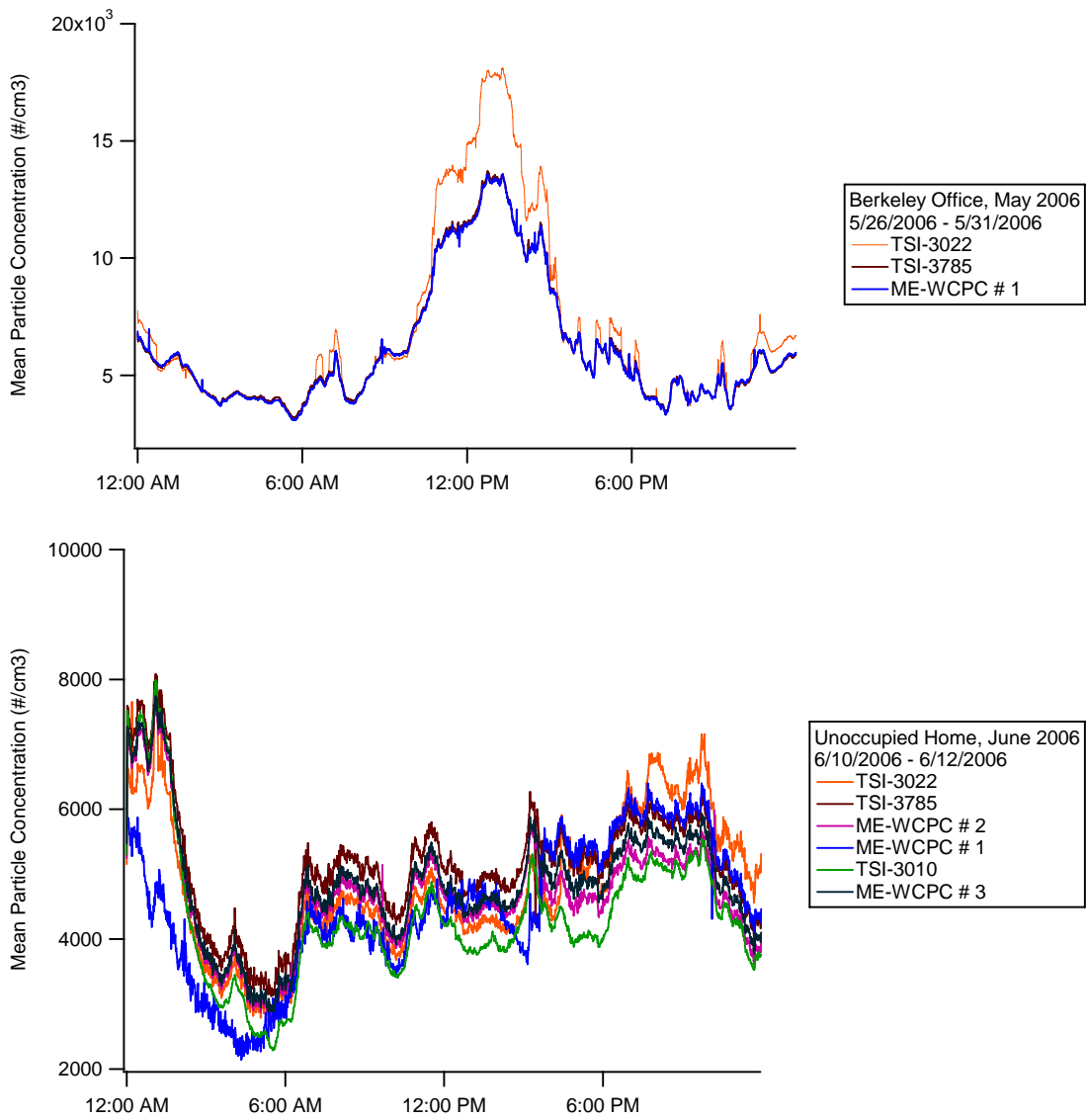


Figure 12. Diurnal patterns in ambient particle number concentrations in an office, and in an unoccupied home in Berkeley, CA, as measured by different condensation particle counters.

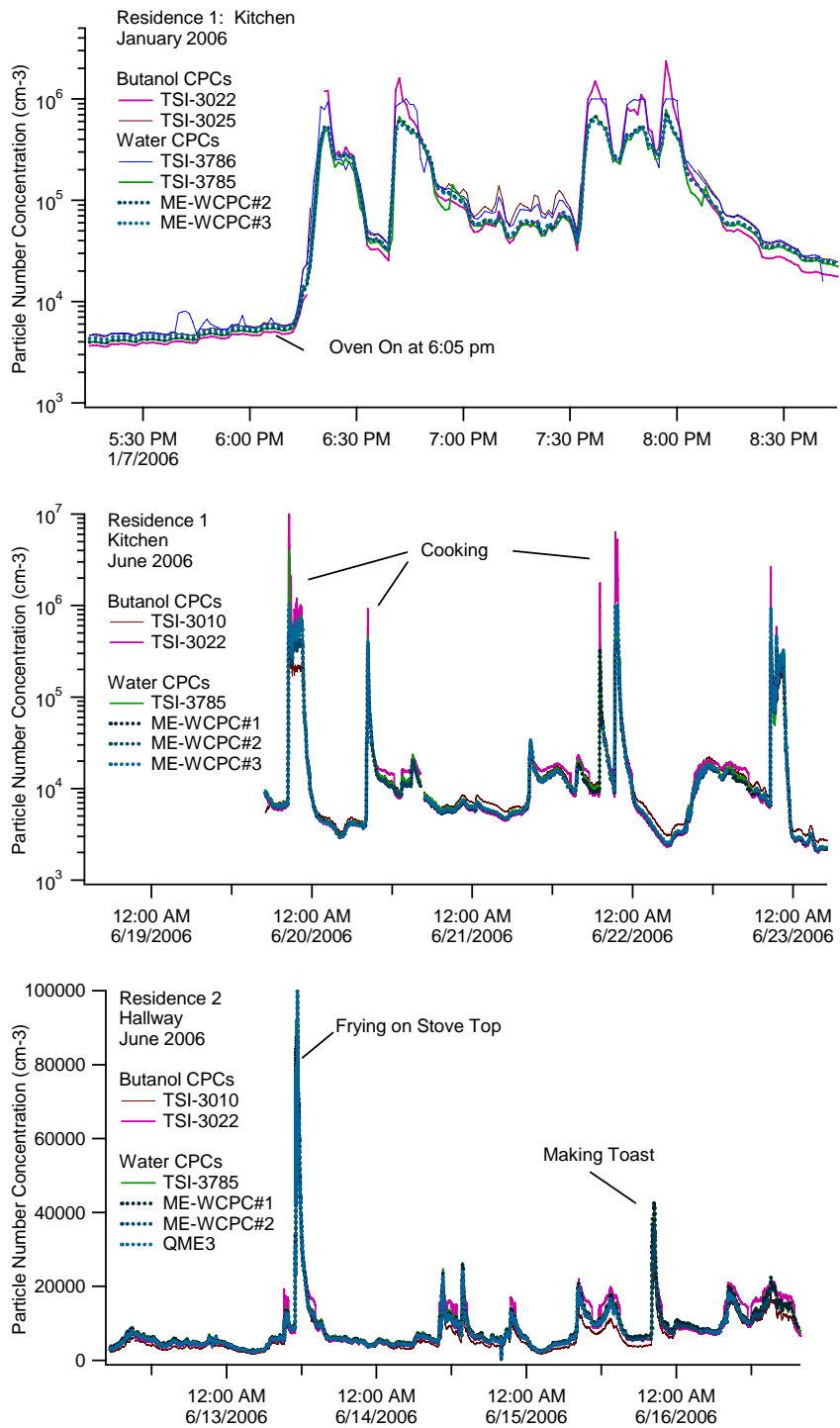


Figure 13. Measurements in a residential kitchen and in a bedroom hallway, showing dramatic increases in particle number concentrations coincident with the use of a gas-fired oven. Data are from the kitchen of Residence 1 (top and middle) and the bedroom wing hallway in Residence 2 (bottom).

is operated. Large concentrations are also seen for operation of an electric toaster, even without the presence of toast. All of the instruments respond to these sources, although discrepancies are seen at the higher concentrations.

Figure 13 (bottom panel) gives data from Residence 2 when it was occupied. At this residence sampling was done from the hallway, in the bedroom area of the house. Overall the concentrations are noticeably higher than for the unoccupied house. An informal log kept by the resident indicates the most pronounced number concentration peaks were associated with cooking activities, with smaller peaks during morning activities. The large maxima midday on 6/13 is from cooking involving frying. As in the ambient data, the concentration among all instruments is well-correlated.

Comparisons Among Instruments

The precision of the ME-WCPC instruments under field conditions is assessed by comparing collocated instruments. A scatter plot of collocated ME-WCPC from the December study in Berkeley is shown in Figure 14. A complete set of plots are attached as Appendix A. Regression results for individual pairwise comparisons are given in Table 3. For all comparisons among ME-WCPC the correlation coefficient $R^2 > 0.97$, and the regression slopes fall between 0.9 and 1.1.

The accuracy of the ME-WCPC is assessed by comparison to the TSI-3022, as this instrument has the closest cutpoint characteristics to the ME units. Data are shown for ambient measurements in Figure 15, with further plots attached as Appendix B. Although at $R^2 > 0.94$ the correlation coefficients are not as consistently high as for collocated sampling, the regression slopes are near one. Table 4 lists results from individual comparisons for all of the ambient measurements.

Table 3. Comparisons for Collocated ME-WCPC Units

	Comparison	Concentration	slope	intercept	R2
Riverside Ambient Measurements					
Summer:	ME-1.vs.ME-2	<60K	0.999 ±0.001	103 ±13	0.991
	ME-3.vs.ME-2	<60K	0.996 ±0.003	63 ±42	0.965
Winter:	ME-2.vs.ME-1	<60K	0.907 ±0.001	24 ±14	0.984
	ME-3.vs.ME-1	<60K	1.083 ±0.001	170 ±8	0.996
Berkeley Ambient Measurements					
Fall	ME-1.vs.ME-2	<180K	1.052 ±0.001	-37 ±8	0.998
	ME-3.vs.ME-2	<180K	1.010 ±0.001	252 ±7	0.999
Winter:	ME-3.vs.ME-2	<180K	0.970 ±0.001	349 ±26	0.989
Indoor Measurements					
Jan '06	ME-3.vs.ME-2	<180K	0.860 ±0.002	2788 ±223	0.989
June '06	ME-1.vs.ME-2	<600K	1.010 ±0.001	94 ±21	0.991
	ME-3.vs.ME-2	<600K	1.345 ±0.001	-2091 ±27	0.991

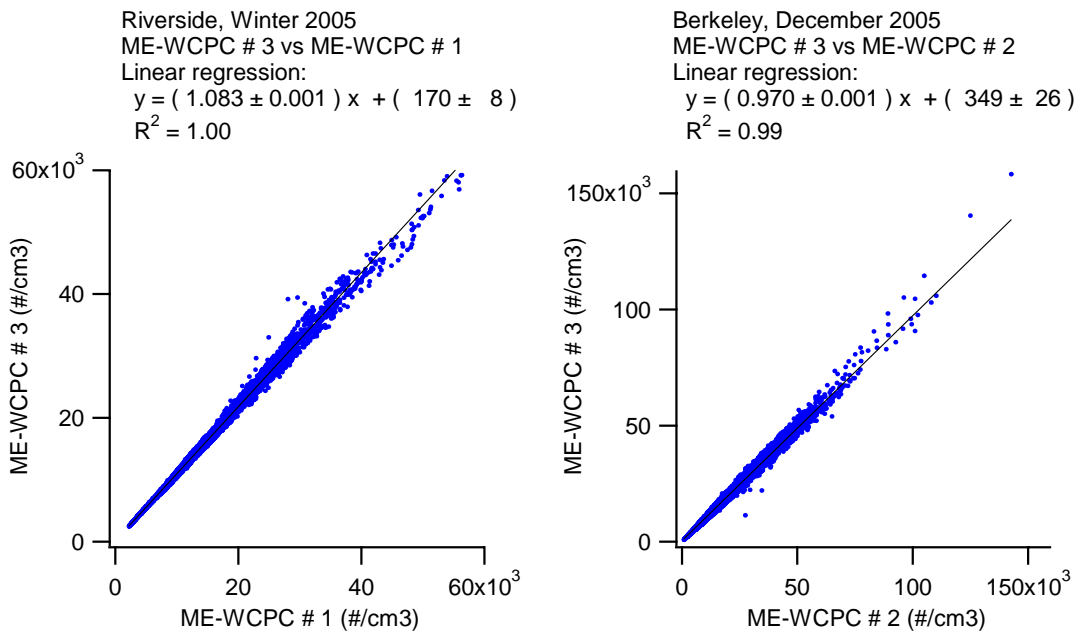


Figure 14. Scatterplots comparing the response of collocated ME-WCPC units during the Riverside and December ambient measurement periods.

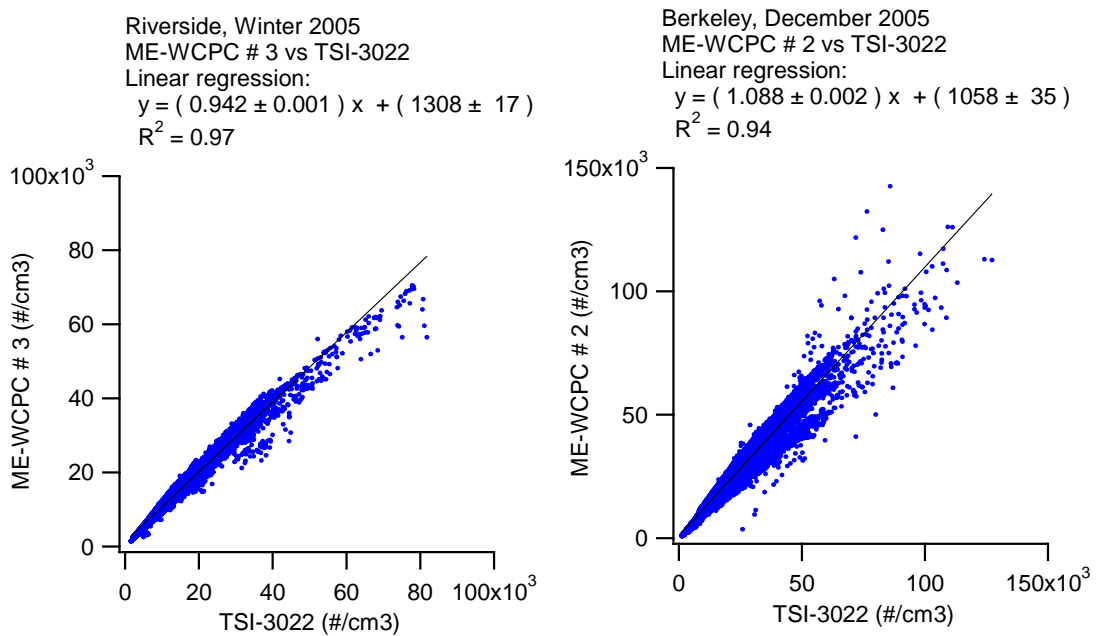


Figure 15. Scatterplots comparing the response the ME-WCPC unit to that of the butanol-based TSI-3022 for ambient measurements in Riverside and Berkeley, California.

Table 4. Pairwise Comparisons Among Instruments

	Range of Concentration	Slope	Intercept	R ²
Summer, Riverside				
ME-1.vs.TSI-3010	<100K	1.136 ±0.002	-988 ±29	0.946
ME-2.vs.TSI-3010	<100K	1.128 ±0.002	-945 ±29	0.937
ME-3.vs.TSI-3010	<100K	1.035 ±0.004	-473 ±51	0.930
ME-2.vs.TSI-3785	<100K	0.989 ±0.001	-1209 ±14	0.986
ME-2.vs.TSI-3025	<100K	0.845 ±0.001	138 ±27	0.943
Winter, Riverside				
ME-1.vs.TSI-3022	<100K	0.901 ±0.001	987 ±18	0.976
ME-2.vs.TSI-3022	<100K	0.771 ±0.001	1209 ±22	0.952
ME-3.vs.TSI-3022	<100K	0.942 ±0.001	1308 ±17	0.973
ME-3.vs.TSI-3010	<100K	0.957 ±0.002	1320 ±28	0.923
ME-3.vs.TSI-3785	<100K	0.868 ±0.001	1013 ±23	0.950
Fall, Berkeley				
ME-1.vs.TSI-3022	<150K	0.947 ±0.002	1146 ±31	0.963
ME-2.vs.TSI-3022	<150K	0.899 ±0.002	1128 ±28	0.965
ME-3.vs.TSI-3022	<150K	0.905 ±0.002	1433 ±33	0.965
ME-3.vs.TSI-3785	<150K	1.177 ±0.005	-1663 ±62	0.931
ME-3.vs.TSI-3025	<150K	0.837 ±0.004	668 ±58	0.881
Winter, Berkeley				
ME-2.vs.TSI-3022	<150K	1.088 ±0.002	1058 ±35	0.941
ME-3.vs.TSI-3022	<150K	1.082 ±0.002	886 ±50	0.958
ME-2.vs.TSI-3010	<150K	1.245 ±0.002	1276 ±37	0.935
ME-2.vs.TSI-3785	<150K	1.067 ±0.001	-496 ±31	0.957
Indoors, Office and Homes				
ME-1.vs.TSI-3022	<200K	0.948 ±0.001	89 ±13	0.967
ME-2.vs.TSI-3022	<200K	0.923 ±0.001	378 ±15	0.965
ME-3.vs.TSI-3022	<200K	0.981 ±0.001	79 ±19	0.957
ME-2.vs.TSI-3010	<200K	1.132 ±0.002	372 ±27	0.893
ME-2.vs.TSI-3785	<200K	0.903 ±0.001	329 ±20	0.936

For measurements in occupied homes, very high concentrations were observed in association with cooking activities. At these high concentrations, consistently higher values are reported by the photometric, butanol-based CPC. For high concentration data, we also examine the dilution-corrected data from the TSI-3010 for the evening of June 23rd, when concentrations fluctuated. For this period the ratio between the TSI-3010 and other instruments was consistent when particle concentrations were low. We inferred a dilution factor of 60 by comparison of reported values at low concentrations. Figure 16 shows the response for concentrations as high as $6 \times 10^5 \text{ cm}^{-3}$, which after dilution corresponds to the upper concentration limit of 10^4 cm^{-3} for the TSI-3010. As is apparent, the TSI-3010 data fall off by comparison with the TSI-3022, in a manner similar to that observed for the ME-WCPC.

A similar comparison at high concentrations is shown in Figure 17 for kitchen measurements conducted in January. Here comparison is made between the ME-WCPC and the TSI-3022 operated with an 8x dilution. In this comparison the two types of instruments agree for concentrations below $600,000 \text{ cm}^{-3}$. Possible reason for differences is a difference in the photometric response of the butanol instrument to ambient and to the salt aerosol with which it is calibrated, and to differences among instruments in the shift of activation efficiencies to larger particle sizes at high particle concentrations due to vapor depletion and condensational heating.

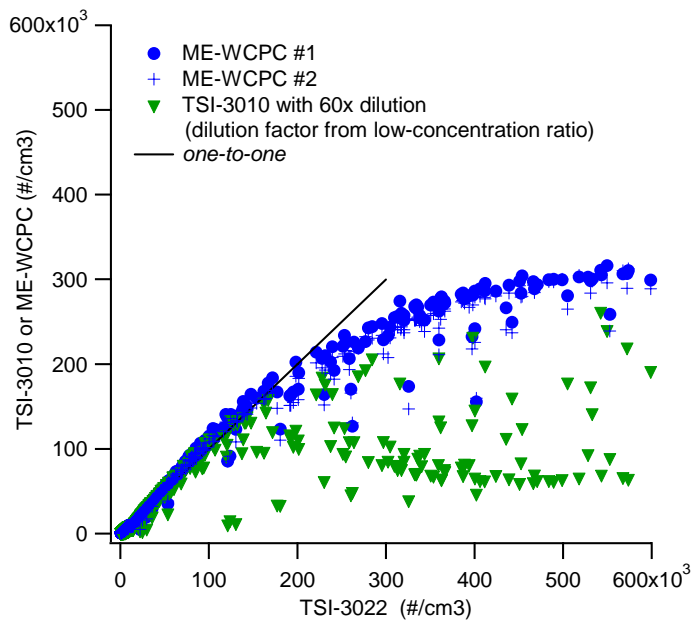


Figure 16. Comparison of the ME-WCPC and the dilution-corrected, single-count mode butanol-based TSI-3010 to the photometric, butanol-based TSI-3022. Data are from a residential kitchen, wherein the TSI-3010 was operated with a passive 60x dilution.

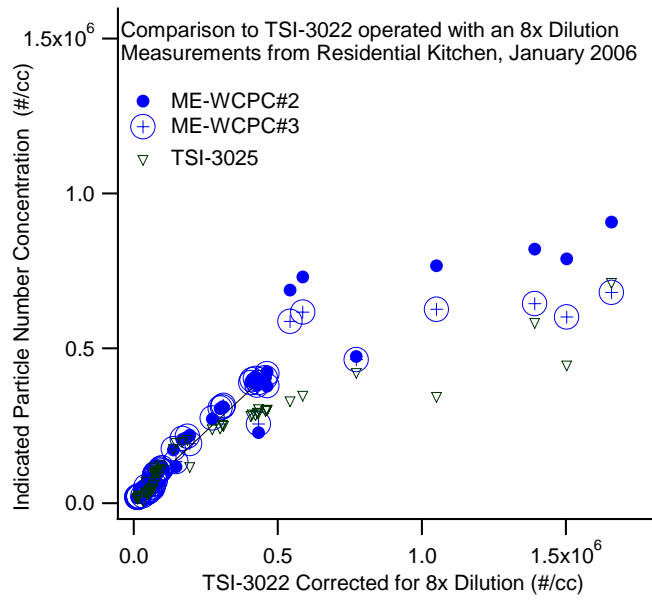


Figure 17. Comparison of the ME-WCPC and the butanol-based TSI-3025 to the TSI-3022 operated with an 8-fold dilution.

Summary

A prototype of a compact, lower-cost, water-based condensation particle counter has been compared to the more widely established butanol-based condensation particle counters under field conditions. Ambient aerosol testing was done in the summer and winter in Riverside, and Berkeley, California. Comparisons for indoor aerosols were made in an occupied office and at two residences.

The ambient data exhibited consistent diurnal pattern during each multi-week study period. All ambient data show a predominant morning maximum in particle number concentration, with a secondary maximum in the afternoon. In some cases, a third maximum is seen shortly after midnight. The data also point to the need to measure in residential and office spaces. The particle number concentrations in these spaces appear to be dominated by indoor, rather than outdoor sources. For the unoccupied residence, the particle number concentrations were much lower than observed outdoors, while those for the occupied residence could be much higher. Residential particle number concentrations associated with cooking activities were larger by a factor of 10 or more than the highest levels observed outdoors.

For both ambient and indoor sampling, the ME-WCPC agreed with butanol instruments at particle concentrations below $200,000 \text{ cm}^{-3}$ with $R^2 > 0.94$ and slopes ranging from 0.90 to 1.08. The precision of the ME-WCPC, was assessed by collocated measurements, and showed correlation coefficient squared of $R^2 > 0.97$, and slopes from 0.9 to 1.1. At higher particle concentrations, there is divergence among the instruments, with the photometrically-based TSI-3022 reporting higher values than either the butanol-based TSI-3010, operated with dilution air, or the ME-WCPCs. Consistent with the goals of the ICAT program, the ME-WCPC has been brought to market, and is sold by TSI as the Model 3781.

References

- 1 Delfino RJ, Sioutas C, Malik S, 2005. Potential role of ultrafine particles in associations between airborne particle mass and cardiovascular health. *Environmental Health Perspectives* 113,934-946.
- 2 Oberdorster, G., Ferin, J., Gelein, R., Soderholm, S.C. and Finkelstein, J., 1992. Role of alveolar macrophage in lung injury; studies with ultrafine particles. *Environmental Health Perspectives* 102, pp. 173–179.
- 3 Oberdorster, G., Gelein, R.M., Ferin, J. and Weiss, B., 1995. Association of particulate air pollution and acute mortality: involvement of ultrafine particles. *Inhalation Toxicology* 7: 111–124.
- 4 Oberdorster, G. (2001). Pulmonary effects of inhaled ultrafine particles. *Int Arch Occup Environ Health*, 74(1) 1-8.
- 5 He C, Morawska L, Hitchins J, Gilbert D, 2004. Contribution from indoor sources to particle number and mass concentrations in residential houses. *Atmospheric Environment* 38, 3405-3415
- 6 Morawska L, He C, Hitchins J, Mengersen K, Gilbert D, 2003. Characteristics of particle number and mass concentrations in residential houses in Brisbane, Australia. *Atmospheric Environment* 37, 4195-4203.
- 7 Morawska, L., Jayarantne, E.R., Mengersen, K. and Thomas, S., 2002. Differences in airborne particle and gaseous concentrations in urban air between weekdays and weekends. *Atmospheric Environment* 36, pp. 4375–4383.
- 8 Wallace L, Howard-Reed C, 2002. Continuous monitoring of ultrafine, fine, and coarse particles in a residence for 18 months in 1999-2000. *Journal of the Air & Waste Management Association* 52, 828-844.
- 9 Wallace LA, Emmerich SJ, Howard-Reed C, 2004a. Source strengths of ultrafine and fine particles due to cooking with a gas stove. *Environmental Science & Technology* 38, 2304-2311.
- 10 Orawska, L. Thomas, S., Gilbert, D., Greenaway C., Rijnders E., (1999) A study of the horizontal and vertical profile of submicrometer particles in relation to a busy road, *Atmospheric Environment* 33: 1261-1274.
- 11 Zhu Y, Hinds WC, Krudysz M, Kuhn T, Froines J, Sioutas C, 2005. Penetration of freeway ultrafine particles into indoor environments. *Journal of Aerosol Science* 36, 303-322.

- 12 Hering S.V. and Stolzenburg, M.R. (2005). *Aerosol Science and Technology* 39: 428-436.
- 13 Hering S.V, Stolzenburg, M.R., Quant, F.R., Oberreit D.R. and Keady, P.B. (2005). *Aerosol Science and Technology* 39: 659-672.
- 14 Hering, Susanne V. Stolzenburg, Mark R., Quant, Frederick R., Oberreit, Derek R. , Keady, Patricia B., A Water-Based, Ultrafine-Particle Concentration Monitor, presented at the Annual Meeting of the American Association for Aerosol Research, October, 2005.
- 15 Stolzenburg, M.R. and McMurry, P.H. (1991) An Ultrafine Aerosol Condensation Nucleus Counter, *Aerosol Science Technology* 14:48-65.

Appendix A.

Scatter plots for comparisons among collocated micro-environmental water condensation particle counters (ME-WCPCs), and between the ME-WCPC and collocated butanol-based condensation particle counters.

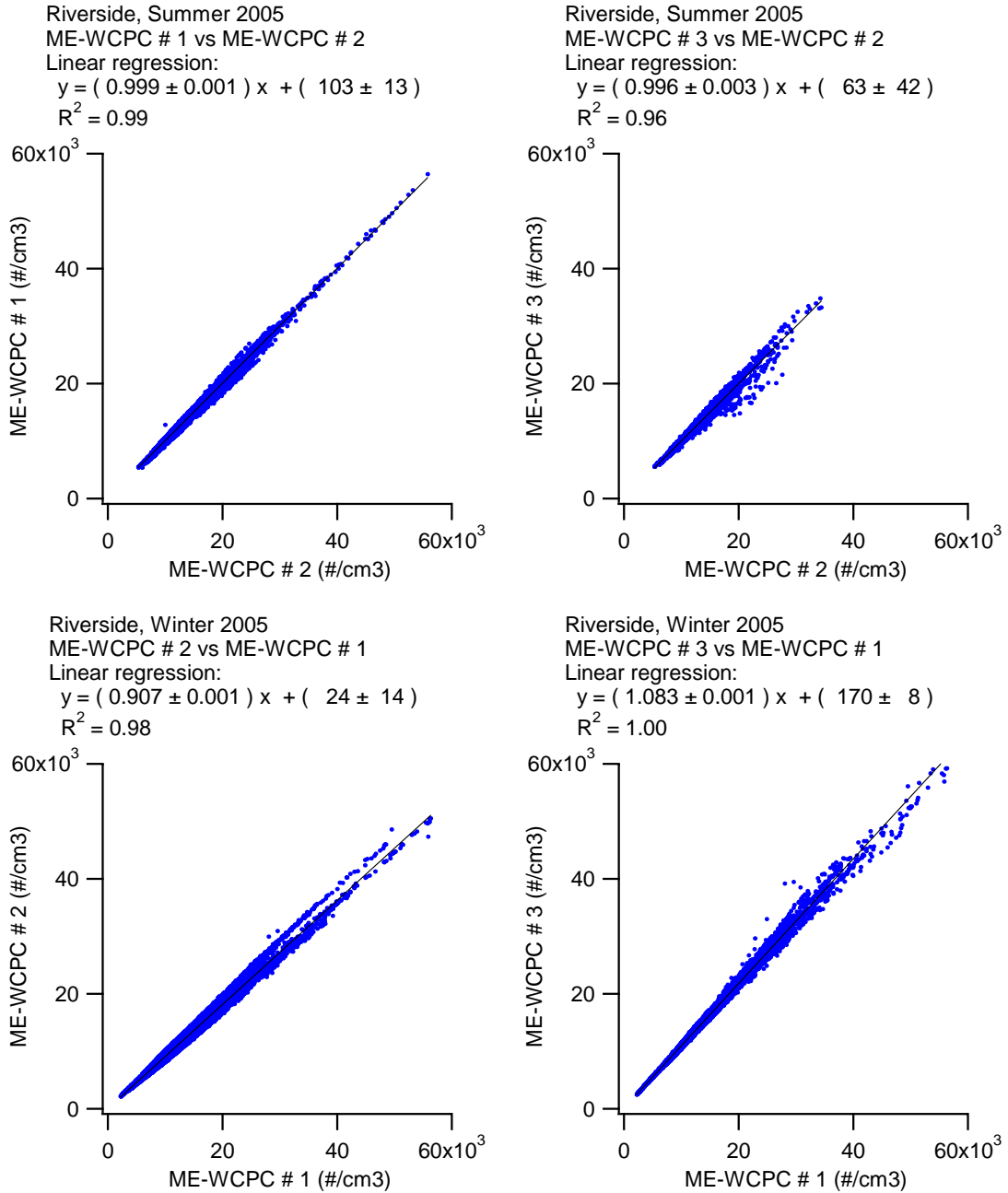
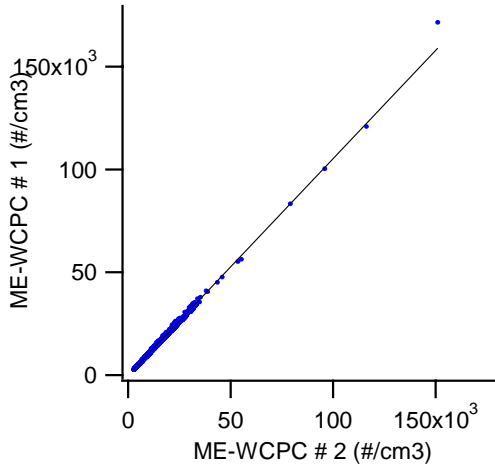
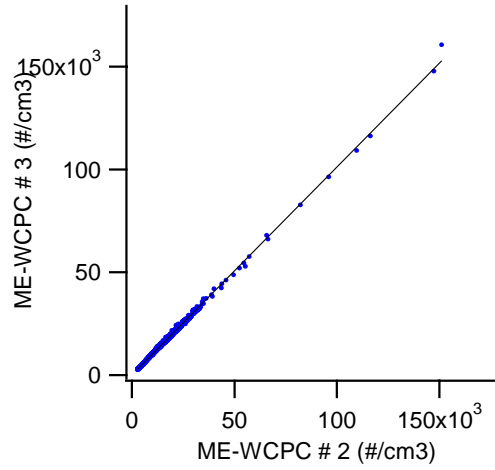


Figure A1. Scatter plots of collocated ME-WCPCs, Riverside Measurements

Berkeley, October 2005
ME-WCPC # 1 vs ME-WCPC # 2
Linear regression:
 $y = (1.052 \pm 0.001) x + (-37 \pm 8)$
 $R^2 = 1.00$



Berkeley, October 2005
ME-WCPC # 3 vs ME-WCPC # 2
Linear regression:
 $y = (1.010 \pm 0.001) x + (252 \pm 7)$
 $R^2 = 1.00$



Berkeley, December 2005
ME-WCPC # 3 vs ME-WCPC # 2
Linear regression:
 $y = (0.970 \pm 0.001) x + (349 \pm 26)$
 $R^2 = 0.99$

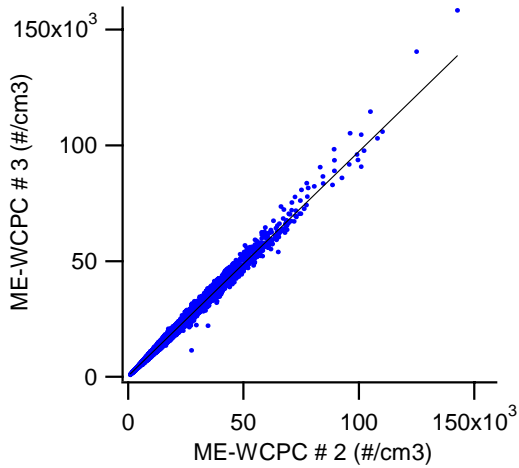


Figure A2. Scatter plots of collocated ME-WCPCs, ambient Berkeley measurements.

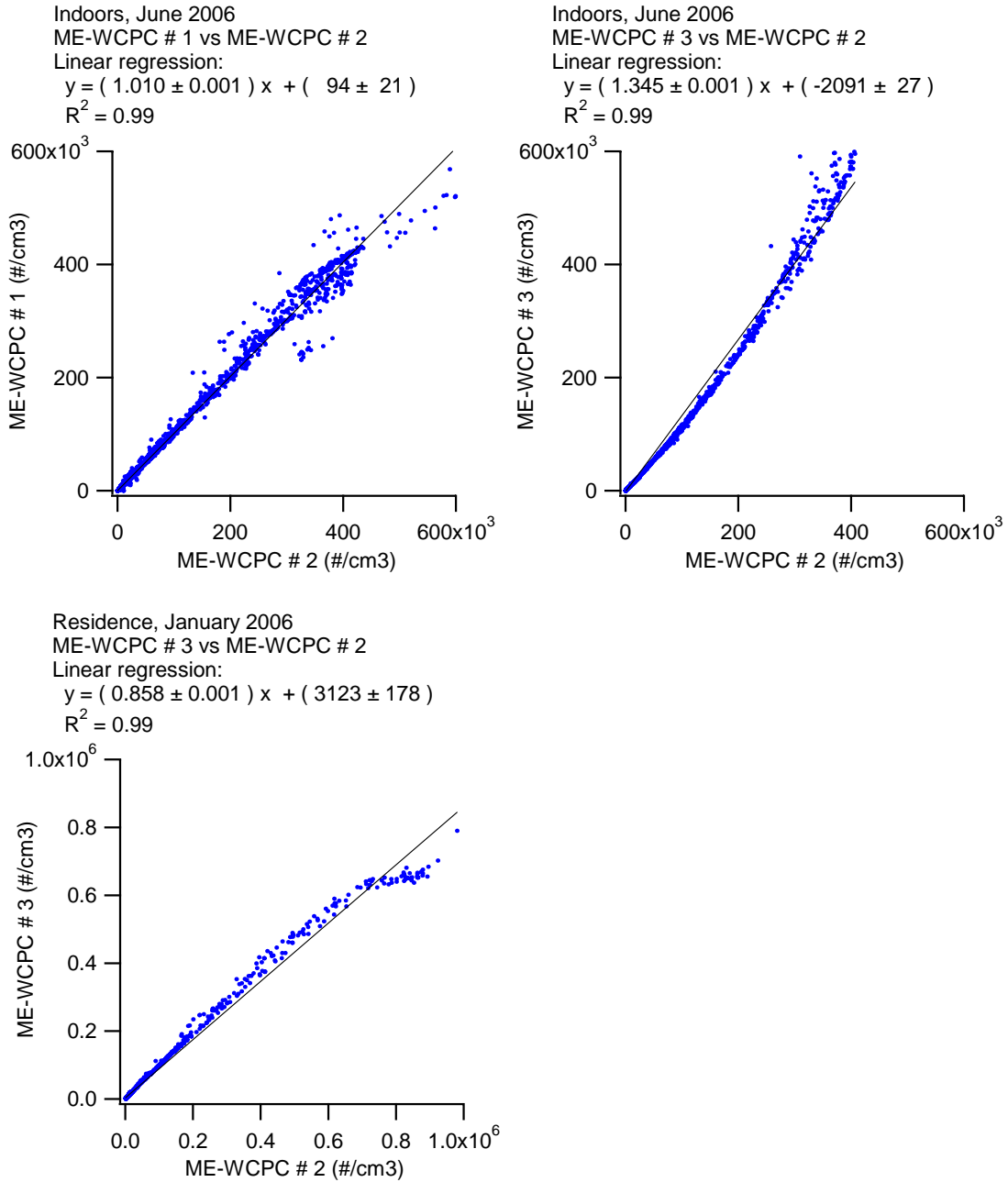


Figure A3. Scatter plots of collocated ME-WCPCs, indoor measurements.

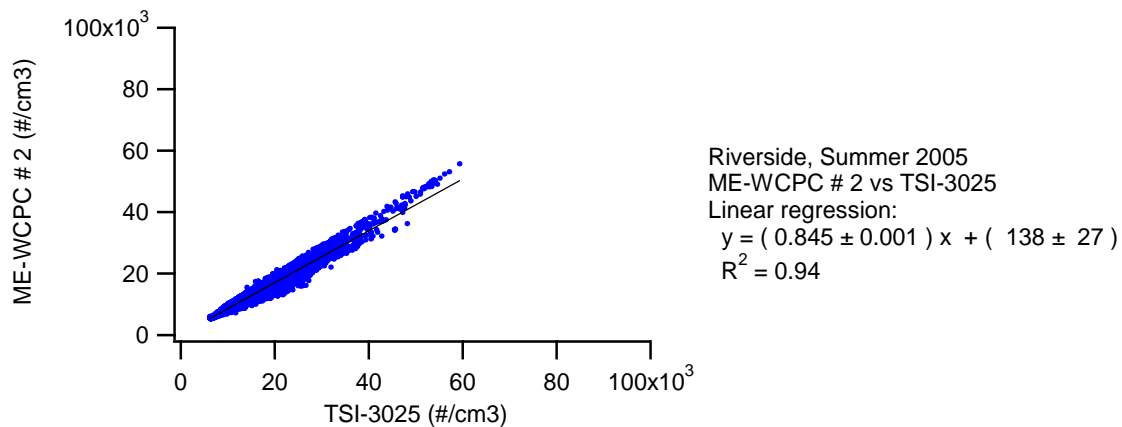
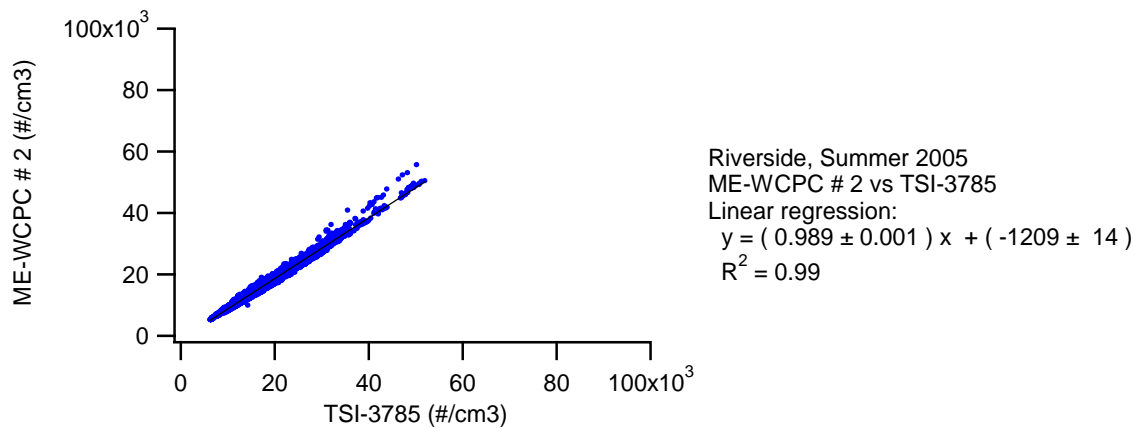
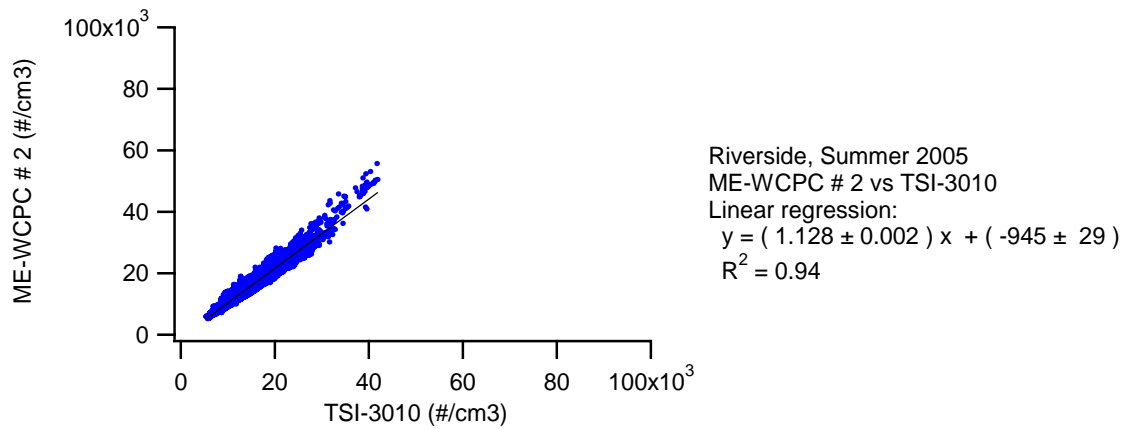


Figure A4. Comparison of the ME-WCPC to butanol CPC for summer time measurements in Riverside.

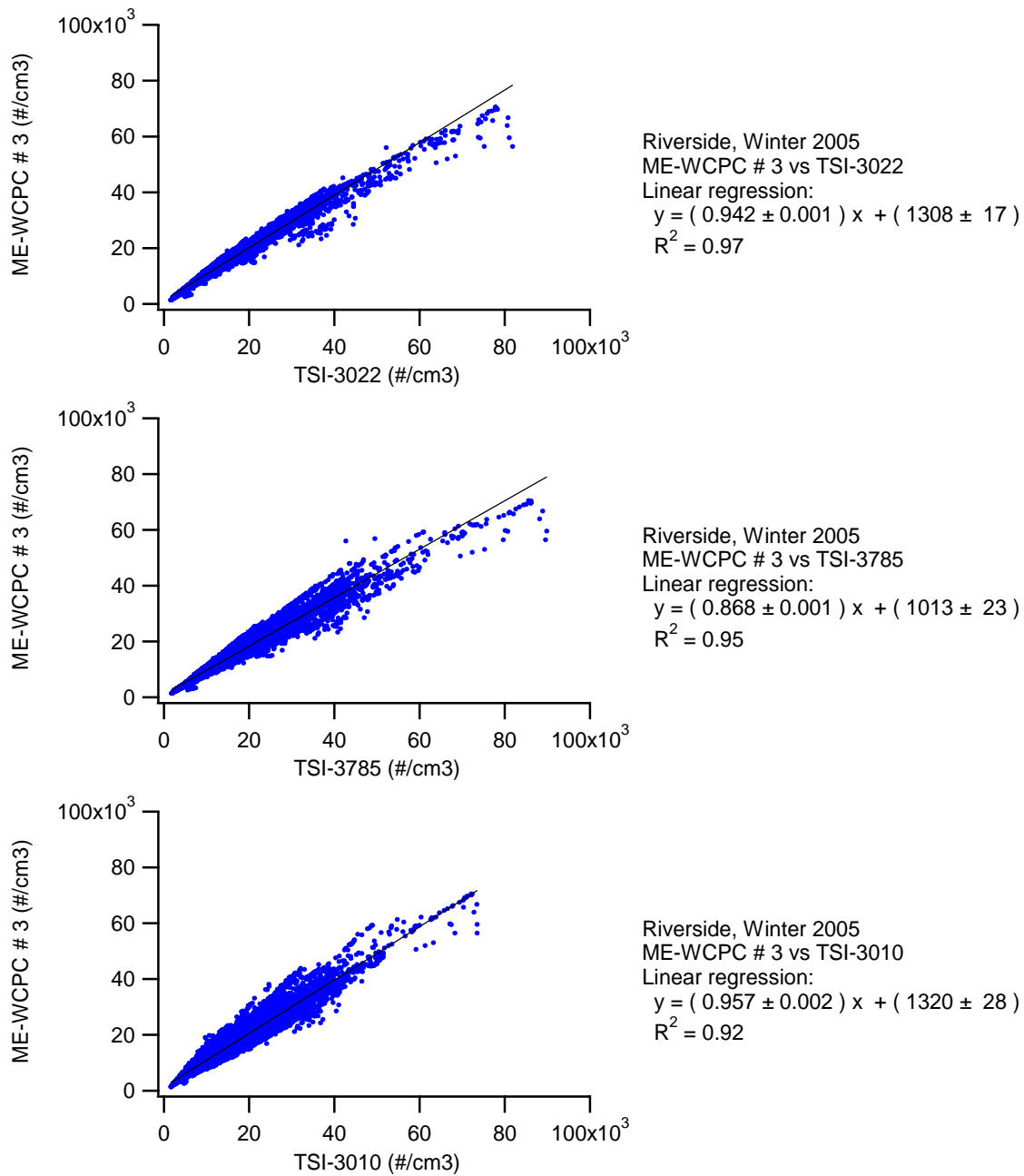
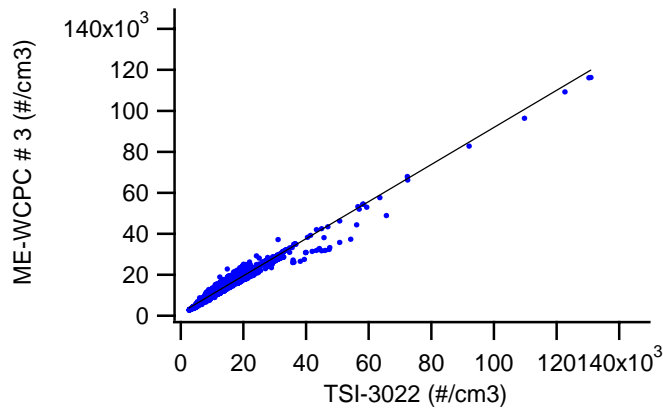
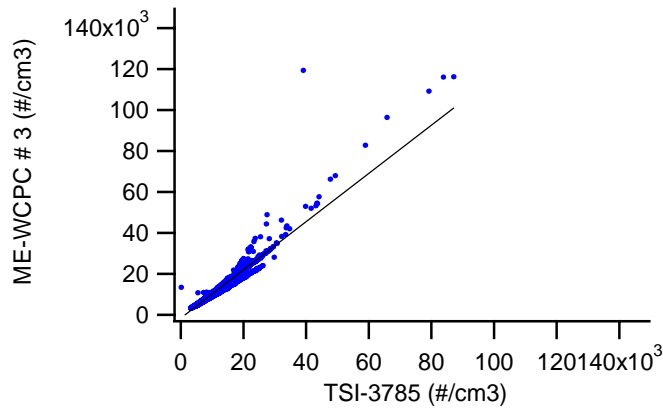


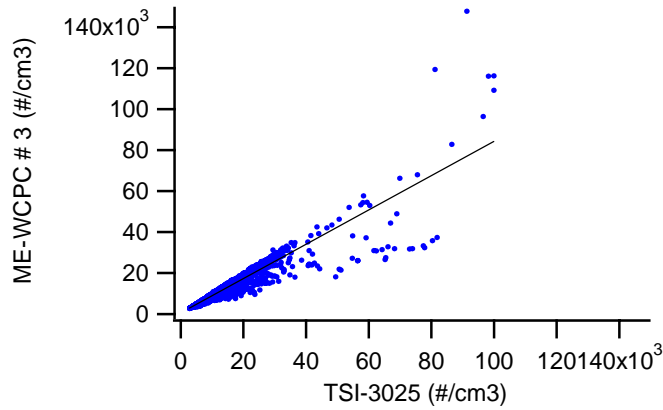
Figure A5. Comparison of the ME-WCPC to butanol CPC for winter measurements in Riverside.



Berkeley, October 2005
 ME-WCPC # 3 vs TSI-3022
 Linear regression:
 $y = (0.905 \pm 0.002) x + (1433 \pm 33)$
 $R^2 = 0.97$

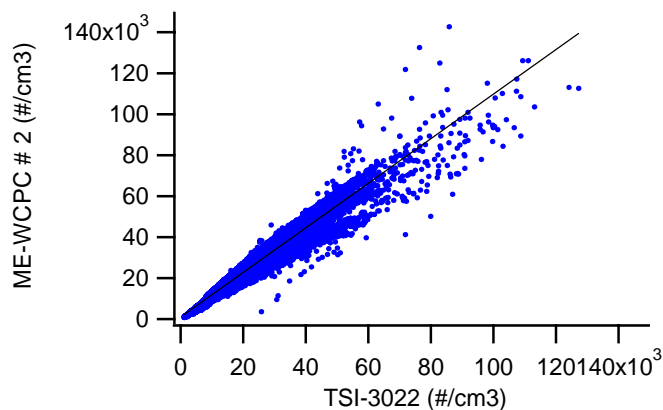


Berkeley, October 2005
 ME-WCPC # 3 vs TSI-3785
 Linear regression:
 $y = (1.177 \pm 0.005) x + (-1663 \pm 62)$
 $R^2 = 0.93$

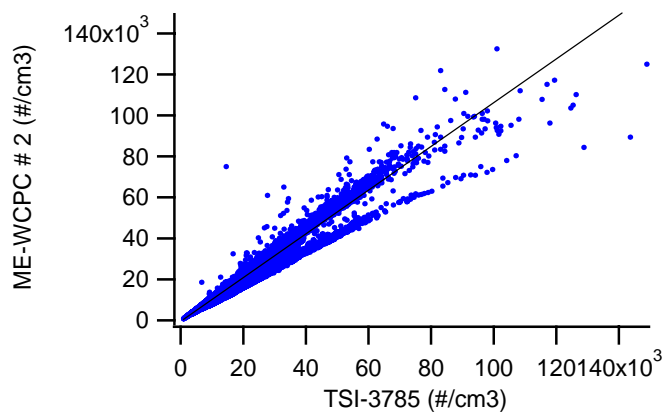


Berkeley, October 2005
 ME-WCPC # 3 vs TSI-3025
 Linear regression:
 $y = (0.837 \pm 0.004) x + (668 \pm 58)$
 $R^2 = 0.88$

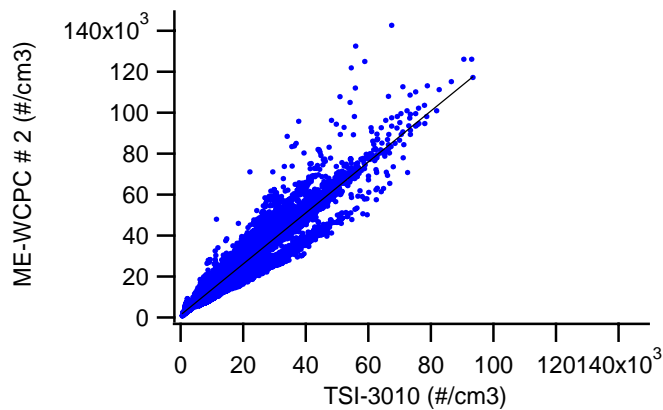
Figure A6. Comparison of the ME-WCPC to butanol CPC for fall measurements in Berkeley.



Berkeley, December 2005
 ME-WCPC # 2 vs TSI-3022
 Linear regression:
 $y = (1.088 \pm 0.002) x + (1058 \pm 35)$
 $R^2 = 0.94$



Berkeley, December 2005
 ME-WCPC # 2 vs TSI-3785
 Linear regression:
 $y = (1.067 \pm 0.001) x + (-496 \pm 31)$
 $R^2 = 0.96$



Berkeley, December 2005
 ME-WCPC # 2 vs TSI-3010
 Linear regression:
 $y = (1.245 \pm 0.002) x + (1276 \pm 37)$
 $R^2 = 0.93$

Figure A7. Comparison of the ME-WCPC to butanol CPC for winter measurements in Berkeley.

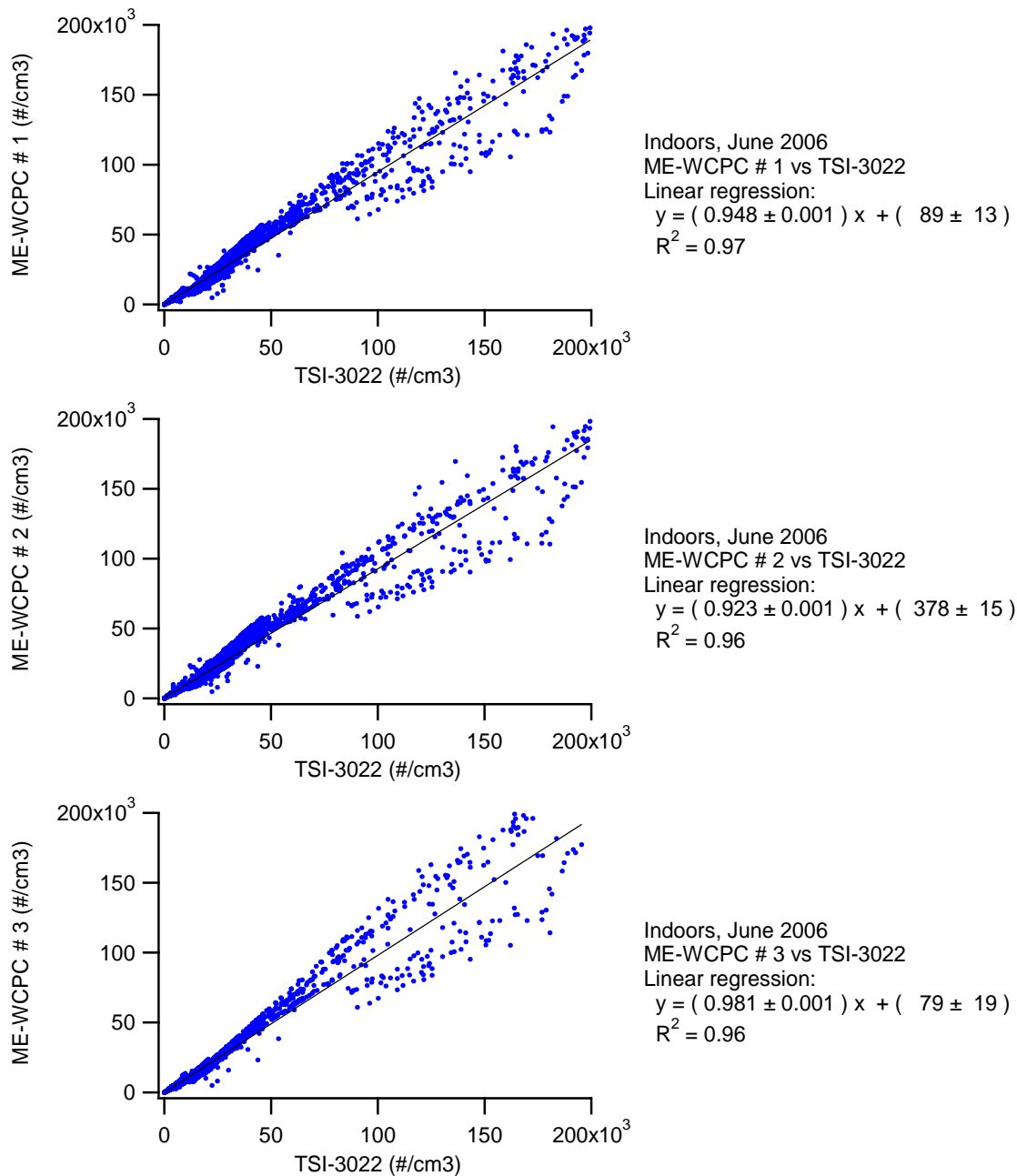


Figure A8. Comparison of the ME-WCPC to butanol CPC for indoor measurements in Berkeley.